

Evolutionary graph theory derived from eco-evolutionary dynamics

Karan Pattni, Christopher E. Overton, Kieran J. Sharkey

karanp@liverpool.ac.uk, c.overton@liverpool.ac.uk, kjs@liverpool.ac.uk
Department of Mathematical Sciences, University of Liverpool

Abstract

A biologically motivated individual-based framework for evolution in network-structured populations is developed that can accommodate eco-evolutionary dynamics. This framework is used to construct a network birth and death model. The evolutionary graph theory model, which considers evolutionary dynamics only, is derived as a special case, highlighting additional assumptions that diverge from real biological processes. This is achieved by introducing a negative ecological feedback loop that suppresses ecological dynamics by forcing births and deaths to be coupled. We also investigate how fitness, a measure of reproductive success used in evolutionary graph theory, is related to the life-history of individuals in terms of their birth and death rates. In simple networks, these ecologically motivated dynamics are used to provide new insight into the spread of adaptive mutations, both with and without clonal interference. For example, the star network, which is known to be an amplifier of selection in evolutionary graph theory, can inhibit the spread of adaptive mutations when individuals can die naturally.

1. Introduction

Evolution is the process by which species adapt and change over time through the basic principles of birth, mutation, interaction and death. It includes ecological dynamics, which is the change in population size and density, and evolutionary dynamics, which is the change in the composition of a given trait in a population. This process is often studied using the assumption of ecological equilibrium, i.e. fixed population size and density or infinite population size, of which examples include classical models [16, 64], adaptive dynamics [12], evolutionary game theory [43, 30, 52], which implements frequency-dependent selection, and evolutionary graph theory [40], which considers a network-structured population. More recent studies consider eco-evolutionary dynamics where ecological and evolutionary dynamics interact [6, 7, 9, 11], which is confirmed to be the case in real biological systems [24, 19]. Our overall objective is to understand how a network-structured population affects eco-evolutionary dynamics. However, our primary focus here is on how ecological dynamics can be suppressed to achieve ecological equilibrium and thereby uncover the hidden ecological assumptions underpinning evolutionary graph theory.

Levins' [39] metapopulation model considers discrete spatial structure in the form of spatially separated sites that can be empty or occupied by a local

population and whose individuals can migrate to other sites. This model has been extended in various ways, for example, by considering a network of sites [26]. Metapopulation models are characterised by their extinction-colonisation dynamics, where local populations on occupied sites can go extinct and unoccupied sites become colonised by migrants. This means that it is possible to have both occupied and unoccupied sites. In structured epidemic models [28, 47], where sites are seen as hosts who can carry infectious disease, the susceptible-infected-susceptible (SIS) dynamics consist of colonisation events in the form of susceptible hosts getting infected and extinction events in the form of infected hosts recovering. In individual-based lattice models, such as the competing contact process [13], sites can accommodate at most one individual, so extinction on a site is a death event and colonisation is a birth event. However, a notable exception is the individual-based framework of evolutionary graph theory [40] where each site always has one individual present on it. Due to this restriction, this framework differs in terms of the dynamics used in the aforementioned models where empty sites are allowed. Dynamics that allow empty sites have been applied to biologically relevant scenarios, for example, in the case of epidemic models: foot-and-mouth disease [36], sexually transmitted diseases [15] and avian influenza [61]. On the other hand, evolutionary graph theory is dominated by theoretical discussions about the importance of population structure on evolution [40, 5, 25]. To bridge the gap between these models, we need to study them within a single framework that will allow us to view their relationship in terms of the underlying biological assumptions made at the individual level.

We construct a modelling framework based on Champagnat et al.’s [6] individual-based model of asexual reproduction. We assume that individuals are distributed over a network of sites such that within a site, the individual-level processes are as described in Champagnat et al. [6] and individuals spread by being dispersed upon birth. Building the framework in this way allows us to use Champagnat et al.’s [6] methods to consider different evolutionary models by changing the timescale of individual-level processes. In the case where mutation rates tend to zero, we are essentially considering only the ecological dynamics; as the mutation rate increases we obtain eco-evolutionary dynamics. In the latter case, we then consider cases where ecological and evolutionary processes happen at similar timescales which, for example, is the case in RNA viruses [23]. Such a framework is particularly useful where network-structure plays an important role. Examples include the spread of antibiotic resistant bacteria around hospital environments [38], and respiratory viruses in human contact networks [59, 63].

The paper is structured as follows. Section 2 describes our framework to model evolution in a network-structured population with eco-evolutionary dynamics based on individual-level processes. Section 3 gives the main result showing that ecological dynamics can be suppressed in our framework’s eco-evolutionary dynamics by using a negative ecological feedback loop. This framework is used in section 4 to construct the network birth and death model (NBD) with ecologically motivated dynamics, which includes the SIS epidemic model [28] as a special case. We then apply the result in section 3 to this model to derive evolutionary graph theory dynamics. In section 5, we investigate the long-term behaviour of the NBD model by calculating the probability of an adaptive mutant replacing a resident population both with and without clonal

interference. We end with a brief discussion.

2. Evolution modelling framework with network structure and eco-evolutionary dynamics

We consider a population in which individuals are distributed over a finite number of connected sites. Individuals and sites represent different things depending on the modelling context. Examples can be found in the metapopulation and epidemiology literature such as the fragmented habitat of fritillary butterflies [27] and farms housing livestock infected with foot and mouth disease [42]. The sites are assumed to be arranged on a network such that individuals can spread to a connected site only. Examples of natural and artificial networks where the spread of individuals is restricted to nearest neighbours include email networks spreading computer viruses [51] and livestock movement networks [37].

The framework describes a birth and death process where the population is updated in continuous time through either a birth or death event, respectively increasing or decreasing the population size by one. Champagnat et al. [6] describes these events at the individual level, incorporating interaction and mutation. Here we follow this approach, but also take into account the site network. For birth events, individuals are assumed to reproduce asexually, giving rise to an offspring that is of identical type when there is no mutation or of a different type when there is mutation. Individuals spread upon birth such that offspring can be placed onto a connected site where they mature immediately and remain until death. Examples of where this type of spreading dynamics can be used include modelling dispersal in plants [17], spread of social behaviour such as alcoholism [58] and spread of infectious disease in epidemics. For death events, it is assumed that individuals free up any space that they previously occupied. Deaths and births are assumed to be independent events allowing the population size and density to fluctuate.

Mutation allows the introduction of a continuous number of new types into the population. In this case, when the evolution of a population is studied over a long period of time, multiple different types can appear that could potentially result in clonal interference [20] where two or more adaptive mutations are in competition with one another. This also allows consideration of a richer adaptive landscape. Interaction between individuals on the same site and potentially different sites as well can affect birth and/or death. In particular, interaction allows the consideration of frequency dependent selection over the adaptive landscape through the use of evolutionary game theory [43, 53, 1].

The mathematical description of the framework is as follows. We consider N distinct sites that are connected to each other in a network. If two sites are connected, then individuals can spread from one to the other. These connections are represented by a matrix W with entries $W_{m,n} \geq 0$, such that sites m and n are connected if $W_{m,n} > 0$. Each site can be occupied by multiple individuals. Let the set of traits be given by $\mathcal{U} \subset \mathbb{R}^l$, i.e. an individual can have l real-valued traits, and let the set of positions individuals can occupy be given by $\mathcal{X} = \{1, 2, \dots, N\}$. Each individual i is then characterised by a separate position and trait such that $i = (U_i, X_i)$ where $U_i \in \mathcal{U}$ is its phenotype and $X_i \in \mathcal{X}$ is its position. This way of characterising individuals is taken from Champagnat & Méléard [8] but here \mathcal{X} is a discrete set. The state of the population at a given point in time is given by the multiset \mathcal{I} containing elements $i = (U_i, X_i)$.

Since \mathcal{I} is a multiset, if both $i = (u, x)$ and $j = (u, x)$ then there are at least two copies of (u, x) in \mathcal{I} . We define the multiset $\mathcal{I}_n = \{i \in \mathcal{I} : X_i = n\}$ to represent the individuals present in site n ; it therefore follows that $\mathcal{I}_n \subseteq \mathcal{I}$. The individual-level processes follow a Poisson process as in Champagnat et al. [6], but in our case the network W can have an impact. The death rate of individual $i \in \mathcal{I}$ is given by $d(i, \mathcal{I}, W)$. The birth rate of individual $i \in \mathcal{I}$ when their offspring is spread to site x is given by $b(i, x, \mathcal{I}, W)$. Since W is constant, we will drop W for brevity, i.e. $d(i, \mathcal{I}) = d(i, \mathcal{I}, W)$ and $b(i, x, \mathcal{I}) = b(i, x, \mathcal{I}, W)$. The probability that an offspring of individual i carries a mutation is $\mu(i)$. The probability that individual i gives birth to an offspring with trait w is given by $M(U_i, w)$ such that $M(U_i, w) = 0$ if $w \notin \mathcal{U}$.

Putting this together gives a model of population evolution described by a continuous time Markov process. The infinitesimal dynamics of the state of the population \mathcal{I} at time t is described by the generator \mathcal{L} that acts on real bounded functions $\phi(\mathcal{I})$ as follows

$$\begin{aligned} \mathcal{L}\phi(\mathcal{I}) = & \sum_{i \in \mathcal{I}} \sum_{n \in \mathcal{X}} [1 - \mu(i)] b(i, n, \mathcal{I}) [\phi(\mathcal{I} \cup \{(U_i, n)\}) - \phi(\mathcal{I})] \\ & + \sum_{i \in \mathcal{I}} \sum_{n \in \mathcal{X}} \mu(i) b(i, n, \mathcal{I}) \int_{\mathbb{R}^t} [\phi(\mathcal{I} \cup \{(w, n)\}) - \phi(\mathcal{I})] M(U_i, w) dw \\ & + \sum_{i \in \mathcal{I}} d(i, \mathcal{I}) [\phi(\mathcal{I} \setminus \{i\}) - \phi(\mathcal{I})]. \end{aligned} \quad (1)$$

The infinitesimal generator describes the way in which the population can change over time. In particular, it describes three different events that can cause the population to change. The event described by the first line is an offspring born with no mutation, the second line is an offspring born with a mutation and the last line represents the death of an individual. For further details on the infinitesimal generator see Appendix A.

In evolutionary dynamics, we are interested in eventually reaching some population state \mathcal{A} from an initial state \mathcal{I} . The probability of this happening is called the hitting probability, denoted $h_{\mathcal{A}}(\mathcal{I})$, and is obtained from the infinitesimal generator by solving

$$\begin{cases} \mathcal{L}h_{\mathcal{A}}(\mathcal{I}) = 0, \\ h_{\mathcal{A}}(\mathcal{A}) = 1. \end{cases} \quad (2)$$

The generator can also be used to find the hitting time. The derivation of the hitting probability and time are in Appendix A.

3. Suppressing ecological dynamics in eco-evolutionary dynamics

We show that we can suppress ecological dynamics in the eco-evolutionary dynamics proposed, leaving us with evolutionary dynamics that are based on ecologically motivated assumptions. In models that only consider evolutionary dynamics, such as the Moran process [49] and evolutionary graph theory [40], these underlying ecological assumptions are lost. This is because their evolutionary dynamics are directly defined from the assumption of fixed population size and density, rather than treating it as a consequence of suppressing ecological dynamics as is the case here.

When ecological dynamics are suppressed, the carrying capacity does not depend upon the composition of the population. To achieve this behaviour, we create a negative ecological feedback loop that balances out opposing ecological forces pushing the system towards an equilibrium. For example, there is negative feedback between predators and their prey where an increase in predators leads to decrease in prey and vice versa [3]. In our framework, the ecological processes that result in a birth oppose those that result in a death. We therefore balance out these processes such that a population converges to a given size regardless of its composition.

The equilibrium we consider is where the population size is N and population density, defined here as the number of individuals per site, is 1. There are several ways available to modify the birth and death rates so that, whenever there is a deviation from the equilibrium, a negative ecological feedback loop comes into effect and pushes the population towards the equilibrium. Due to its simplicity, we have opted to use the Heaviside step function

$$H_y[z] = \begin{cases} 0 & z < y, \\ 1 & z \geq y. \end{cases}$$

The modified death rate of individual i amplifies its death rate by c if present on a site with multiple occupancy but otherwise has no effect; that is,

$$D(c, i, \mathcal{I}) = c^{H_2[\|\mathcal{I}_{x_i}\|]} d(i, \mathcal{I}) \quad c \geq 1. \quad (3)$$

Similarly, the modified birth rate of individual i amplifies its birth rate onto site n by c if site n is empty but otherwise has no effect; that is,

$$B(c, i, n, \mathcal{I}) = c^{H_0[-\|\mathcal{I}_n\|]} b(i, n, \mathcal{I}) \quad c \geq 1. \quad (4)$$

The infinitesimal generator for the modified birth and death rates, denoted \mathcal{L}_c , is given by equation (1) but with b replaced by B and d replaced by D . The parameter c controls the strength of the negative ecological feedback loop's effect. For $c = 1$, there is no effect. For $c > 1$, it is more likely that individuals sharing a site will die and that offspring are placed onto empty sites. This effect is maximised for $c \rightarrow \infty$, which suppresses ecological dynamics resulting in fixed population size and density.

When ecological dynamics are suppressed, the system updates through a replacement event where a birth and a death are coupled. This is formally shown by considering the hitting probability. Using the generator \mathcal{L}_c , the hitting probability in the limit as $c \rightarrow \infty$ of the eco-evolutionary dynamics can be shown (Appendix B) to reduce to

$$\begin{aligned} h_{\mathcal{A}}(\mathcal{I}) = & \frac{1}{\lambda_{\mathcal{I}}} \sum_{i \in \mathcal{I}} \sum_{j \in \mathcal{I}} r(i, j, U_i, \mathcal{I}) [1 - \mu(i)] h_{\mathcal{A}}(\mathcal{I} \cup \{(U_i, X_j)\} \setminus \{j\}) \\ & + \int_{\mathbb{R}^l} r(i, j, w, \mathcal{I}) \mu(i) h_{\mathcal{A}}(\mathcal{I} \cup \{(w, X_j)\} \setminus \{j\}) M(U_i, w) dw \end{aligned} \quad (5)$$

where $\lambda_{\mathcal{I}}$ is the rate of leaving state \mathcal{I} and $r(i, j, u, \mathcal{I})$ is the rate at which individual i 's offspring of type u replaces individual j in state \mathcal{I} . This shows that in the limiting dynamics we have derived, the population is updated through

replacement events that happen with rate r . It is shown in Appendix B that the replacement rate r for equation (5) is given by

$$r(i, j, u, \mathcal{I}) = b(i, X_j, \mathcal{I}) \frac{d(j, \mathcal{J})}{\sum_{k \in \mathcal{J}_{X_j}} d(k, \mathcal{J})} + d(j, \mathcal{I}) \frac{b(i, X_j, \mathcal{I} \setminus \{j\})}{\sum_{k \in \mathcal{I} \setminus \{j\}} b(k, X_i, \mathcal{I} \setminus \{j\})} \quad (6)$$

where $\mathcal{J} = \mathcal{I} \cup \{(u, X_j)\}$. We can see in r that there are two components, birth-death (BD), i.e. birth followed by death, and death-birth (DB), i.e. death followed by birth. The first term is a birth-death (BD) component where individual i first gives birth to an offspring that is placed onto site X_j who then replaces individual j . The second term is a death-birth (DB) component where individual j dies first and then individual i gives birth to an offspring that is placed onto site X_j , hence replacing individual j .

4. Framework Application I: Deriving evolutionary graph theory dynamics from a network birth and death process

Here, we construct a model from our framework by using ecologically motivated dynamics, which we will refer to as the network birth and death model (NBD). This model contains the SIS epidemic model [28] and competing contact process [13] as special cases. By suppressing ecological dynamics in eco-evolutionary dynamics as shown in section 3, this model gives evolutionary dynamics based on birth and death rates. By comparing these evolutionary dynamics with evolutionary graph theory which are based on fitness, we show how fitness can be interpreted in terms of birth and death rates, uncovering hidden assumptions and providing biological insight into evolutionary graph theory dynamics.

The intra-site ecological dynamics for NBD uses density-dependent regulation of population size based on Huang et al. [32]. Individuals on the same site compete for survival captured through pairwise interactions resulting in the death of an individual. This competition has negative feedback such that increasing population size results in increased competition and vice versa. For individual i , let δ_{U_i} be the natural death rate and γ_{U_i, U_j} be the death rate due to competition with individual j . Huang et al. [32] specifies that the inverse of γ can be interpreted as the payoff in a game in evolutionary game theory [43]. That is, a larger payoff is received when γ is lower. The death rate is then given by

$$d(i, \mathcal{I}) = \delta_{U_i} + \sum_{j \in \mathcal{I}_{X_i} \setminus \{i\}} \gamma_{U_i, U_j} \quad (7)$$

where self-interactions have been discounted. It is assumed that $\gamma_{u,v} > 0 \forall u, v \in \mathcal{U}$ to ensure negative feedback. The birth rate is given by

$$b(i, n, \mathcal{I}) = s^{|\mathcal{I}_n|} \beta_{U_i} W_{X_i, n} \quad s \in [0, 1]. \quad (8)$$

The birth rate of individual i is β_{U_i} . It is weighted by $W_{X_i, n}$ to capture the network effect of its position when placing its offspring in site n . We added $s^{|\mathcal{I}_n|}$ to capture the ability of an offspring to survive when invading site n depending

on its occupancy. For $0 < s < 1$, there is negative feedback such that survival decreases as occupancy increases and vice versa. For $s = 0$, the convention that $0^0 = 1$ is used implying that there is no invasion because offspring do not survive on occupied sites. For $s = 1$, offspring always survive when invading.

NBD forms a basis for the susceptible-infected-susceptible (SIS) epidemic model [28] and its various extensions. The SIS model captures the ecological dynamics of an infection as it spreads between hosts. A host can be infected (I) or susceptible (S) and is represented by a node in a network. Infection can only spread from an infected to a susceptible. Becoming infected is therefore proportional to the number of infected neighbours, whereas infected individuals recover and become susceptible independent of their neighbours. SIS dynamics generally consider a single pathogen type, but multi-species SIS-type dynamics are obtained from NBD as follows. Each site is a host, with a vacant site representing S and an occupied site representing I. The presence of individual i on a site indicates having infection U_i , i.e. the trait of individual i . The death rate in equation (7) represents recovery from infection and is given by

$$d(i, \mathcal{I}) = \delta_{U_i} \quad (9)$$

where we have set $\gamma_{u,v} = 0$ for all $u, v \in \mathcal{U}$ since the recovery process in SIS dynamics is independent of other infections a host may have. That is, recovery from infection U_i happens with rate δ_{U_i} . The birth rate in equation (8) represents spread of infection and is given by

$$b(i, n, \mathcal{I}) = 0^{|\mathcal{I}_n|} \beta_{U_i} W_{X_i, n} \quad (10)$$

where we have set $s = 0$ to restrict the spread of infection to S (vacant sites) only. Infection U_i spreads with rate β_{U_i} and is weighted by $W_{X_i, n}$ to capture the effect of the network. Constructing the SIS model using NBD allows us to consider extensions that have eco-evolutionary dynamics. A straightforward extension is the competing contact process [13]. This uses SIS dynamics to study inter-host competition where two different infections are competing to occupy hosts. Other extensions such as Beutel et al. [4] allow hosts to carry more than one infection. Here, there is intra-host competition where infections compete within a host. In our setting, this can be achieved when $s > 0$. Therefore, NBD allows us to consider a combination of inter and intra-host competition between infections.

In the framework known as evolutionary graph theory [40, 62], one considers a population of fixed size in which each vertex contains a single individual. We wish to investigate whether such a model can be obtained from the NBD eco-evolutionary dynamics. To do this, we first suppress ecological dynamics (see section 3) to obtain NBD evolutionary dynamics. The replacement rate for NBD evolutionary dynamics is obtained by substituting equations (7) and (8) into equation (6), giving

$$r(i, j, u, \mathcal{I}) = s \beta_{U_i} W_{X_i, X_j} \frac{\delta_{U_j} + \gamma_{U_j, u}}{\delta_{U_j} + \gamma_{U_j, u} + \delta_u + \gamma_{u, U_j}} + \delta_{U_j} \frac{\beta_{U_i} W_{X_i, X_j}}{\sum_{k \in \mathcal{I} \setminus \{j\}} \beta_{U_k} W_{X_k, X_j}}. \quad (11)$$

The exponent of s is 1 in the BD component as every site has one individual in this case. The hitting probability in NBD, denoted $h_A^{\text{NBD}}(\mathcal{I})$, is given by

substituting this replacement rate into equation (5). On the other hand, let $R(i, j, u, \mathcal{I})$ be the replacement rate for evolutionary graph theory dynamics, such that it is the rate at which individual i 's offspring of type u replaces individual j in state \mathcal{I} . Then R will be used to define an infinitesimal generator for evolutionary graph theory and used to solve equation (A.1) to obtain the hitting probability in evolutionary graph theory, denoted $h_{\mathcal{A}}^{\text{EGT}}(\mathcal{I})$. The infinitesimal generator used and hitting probability obtained for evolutionary graph theory are in Appendix C. For equivalence between NBD evolutionary dynamics and evolutionary graph theory dynamics, we check whether they have the same hitting probabilities, i.e. $h_{\mathcal{A}}^{\text{NBD}}(\mathcal{I}) = h_{\mathcal{A}}^{\text{EGT}}(\mathcal{I})$. For the comparisons we make, we consider standard evolutionary graph theory definitions of the replacement rate R .

In evolutionary graph theory, three families of dynamics are generally considered [60]; link (L), death-birth (DB), and birth-death (BD) dynamics. In link dynamics a link in the network is selected, then the offspring of the individual at the start of the link replaces the individual at the end of the link. In death-birth (birth-death) an individual is first selected for death (birth) before a neighbouring individual is selected for birth (death). Each of these families have two distinct cases [55], where individuals are selected for either birth or for death. For link dynamics we will use LB (LD) to indicate selection on birth (death). For BD and DB dynamics, we use an upper case letter to indicate the event in which selection happens [29], e.g. bD indicates selection on death. Selection is dependent on the fitness of the individuals. In evolutionary game theory, fitness is the average payoff received by an individual. Payoffs depend upon the strategy played in a game specifying the rules of interactions between individuals. Here we consider the case where fitness is constant, i.e. it does not depend upon the interactions with other individuals. The fitness of individual i will be denoted F_{U_i} and is assumed to be independent of its site. The replacement rates for the standard evolutionary graph theory dynamics are given in Table 1 and only hold for those states where population density is 1, i.e. for \mathcal{I} such that $|\mathcal{I}|_x = 1 \ \forall x \in \mathcal{X}$.

The conditions required to obtain the standard evolutionary graph theory dynamics from NBD evolutionary dynamics are summarised in Table 2, excluding bD dynamics which could not be obtained. Details are given in Appendix D. The conditions specify whether s, β, δ, γ are suppressed, identical for all traits, proportional to fitness and subject to other requirements. With the exception of LD dynamics, these conditions extend to the case where fitness is not constant such that it could depend upon the system state and not just the trait of an individual. The following insights are obtained from deriving the dynamics in this way:

- Standard evolutionary graph theory dynamics use only one component of NBD evolutionary dynamics. Dynamics using the BD component are obtained by suppressing the natural death rate by setting $\delta_u = 0 \ \forall u \in \mathcal{U}$. This can be viewed as a biological scenario where individuals rarely die naturally but undergo intense intra-site competition with invaders. Individuals that can successfully invade are therefore more likely to spread. Fitness is interpreted as the birth rate when it acts on birth. The inverse fitness is interpreted as the death rate due to competition when it acts on death. On the other hand, dynamics using the DB component are obtained

Table 1: Standard evolutionary graph theory dynamics. The shorthand notation for BD and DB dynamics follows Hindersin & Traulsen [29] where a capital letter is used to indicate whether selection is on birth or death.

Dynamics	Description	$R(i, j, u, \mathcal{I})$
Death-Birth-Death (Db)/Voter Model	Individual j dies inversely proportional to its fitness and is replaced by neighbour i with probability proportional to W_{X_i, X_j} .	$\frac{1/F_{U_j}}{\sum_{n \in \mathcal{I}} 1/F_{U_n}} \frac{W_{X_i, X_j}}{\sum_{k \in \mathcal{I} \setminus \{j\}} W_{X_k, X_j}}$
Death-Birth-Birth (dB)	Individual j dies uniformly at random, i.e. with probability $1/N$, and is then replaced by neighbour i with probability proportional to $F_{U_i} W_{X_i, X_j}$.	$\frac{1}{N} \frac{F_{U_i} W_{X_i, X_j}}{\sum_{k \in \mathcal{I} \setminus \{j\}} F_{U_k} W_{X_k, X_j}}$
Link-Birth (LB)	Individual i replaces j with probability proportional to $F_{U_i} W_{X_i, X_j}$.	$\frac{F_{U_i} W_{X_i, X_j}}{\sum_{n, k \in \mathcal{I}} F_{U_n} W_{X_n, X_k}}$
Link-Death (LD)	Individual i replaces j with probability proportional to $W_{X_i, X_j}/F_{U_j}$.	$\frac{W_{X_i, X_j}/F_{U_j}}{\sum_{n, k \in \mathcal{I}} W_{X_n, X_k}/F_{U_k}}$
Birth-Death-Birth (Bd)/Invasion Process	Individual i is chosen proportional to fitness, then replaces a neighbour j with probability proportional to W_{X_i, X_j} .	$\frac{F_{U_i}}{\sum_{n \in \mathcal{I}} F_{U_n}} \frac{W_{X_i, X_j}}{\sum_{k \in \mathcal{I}} W_{X_i, X_k}}$
Birth-Death-Death (bD)	Individual i is selected uniformly at random who then replaces neighbour j proportional to $W_{X_i, X_j}/F_{U_j}$.	$\frac{1}{N} \frac{W_{X_i, X_j}/F_{U_j}}{\sum_{k \in \mathcal{I}} W_{X_i, X_k}/F_{U_k}}$

Table 2: Assumptions required for all $u, v \in \mathcal{U}$ to obtain standard evolutionary graph theory dynamics from the replacement dynamics. bD dynamics are not listed as they could not be obtained. $\mathbf{1}$ is a column vector of 1s.

Dynamics	Suppressed	Identical	Proportional to Fitness	Other
LB	$\delta_u = 0$	$\gamma_{u,v} = \gamma_{v,u}$	$\beta_u = F_u$	$s > 0$
LD	$\delta_u = 0$	$\beta_u = \beta_v$	$\gamma_{u,v} = 1/F_u, u \neq v$	$s > 0, \mathcal{U} = 2, \mu(i) = 0$
Bd	$\delta_u = 0$	$\gamma_{u,v} = \gamma_{v,u}$	$\beta_u = F_u$	$s > 0, W\mathbf{1} = \mathbf{1}$
Db	$s = 0$	$\beta_u = \beta_v$	$\delta_u = 1/F_u$	–
dB	$s = 0$	$\delta_u = \delta_v$	$\beta_u = F_u$	–

when offspring cannot survive on occupied sites ($s = 0$). Biologically, this can be viewed as invasion being difficult, hence individuals that can outlive their competitors are more likely to spread. Inverse fitness is interpreted as the natural death rate when it acts on death. Fitness is interpreted as the birth rate when it acts on birth.

- Link dynamics is a type of BD dynamics. In their definitions in Table 1, the order of birth and death is ambiguous and so they are classified separately from BD and DB dynamics. This means that intra-site competition also takes place in link dynamics. In LB dynamics intra-site competition is independent of fitness with both individuals equally likely to die. In LD dynamics an individual dies inversely proportional to fitness due to intra-site competition.
- bD dynamics cannot be obtained from NBD evolutionary dynamics. It requires birth and movement to be separate, as is evident in its definition (Table 1) where the term representing birth does not specify where an offspring is placed. Birth and movement is combined in our framework as seen in equation (1) where $b(i, n, \mathcal{I})$ specifies the individual that gives birth and where the offspring is placed.
- Bd dynamics can be obtained from NBD evolutionary dynamics. Similar to bD dynamics, it is also defined with separate birth and movement (Table 1), but its movement term is independent of neighbours. This allows us to combine movement with birth provided that it does not affect birth. This is only true when W is right stochastic ($W\mathbf{1} = \mathbf{1}$) and in this case, Bd and LB are equivalent [55] and therefore share the same spreading mechanism. This is not the case when W is not right stochastic because LB allows position to affect the birth rate, which is $\beta_{U_i} \sum_{x \in \mathcal{X}} W_{X_i, x}$ for i , whereas it is β_{U_i} in Bd which is independent of position.
- Db and dB can be obtained from SIS-type epidemic dynamics. This is because they share the same spreading mechanism and do not have intra-site competition. They are obtained by letting $\beta_u \rightarrow \infty \forall u \in \mathcal{U}$ in equation (10), resulting in vacant sites immediately being occupied by offspring. This is how Durrett & Levin [14] use the contact process to obtain the

voter model [31], which has identical dynamics to Db. This illustrates that pathogen evolution, at least at the between host level, is likely to behave similarly to death-birth evolutionary dynamics rather than birth-death.

- When Db and dB are derived from NBD evolutionary dynamics there is no self-replacement, which means that an individual cannot be replaced by its own offspring. This is because the DB component of NBD evolutionary dynamics specify that death happens first followed by birth, preventing self-replacement. The standard definitions (Table 1) allow self-replacement for both BD and DB type dynamics, but for dynamics derived from NBD evolutionary dynamics this is only possible for BD type dynamics. Note that Db can be obtained from our derivation of LD when W is left stochastic, i.e. $W^T \mathbf{1} = \mathbf{1}$. In this case self-replacement is allowed as LD is a type of BD dynamics. However, using this definition is limited due to the restrictions on LD (see Table 2).

Other non-standard evolutionary graph theory definitions of the replacement rate R can also be considered. For example, Zukewich et al. [65] combines Bd and Db using a parameter to allow a smooth transition between the two. Setting the parameter to 1 gives Bd, 0 gives Db and a value in the 0 to 1 range gives a combination of them. NBD evolutionary dynamics provide a biologically motivated alternative to constructing hybrid models comprising both Bd and Db dynamics. Another example is Kaveh et al.'s [35] DB dynamics that are not based on fitness and are obtained from NBD evolutionary dynamics by setting $s = 0$ in equation (11). They use parameters similar to δ and β that give the likelihood of birth and death. However, their parameters are weights rather than rates since their system is constructed in discrete time.

5. Framework Application II: Long-term behaviour of a network birth and death process

Here we analyse the long-term behaviour of the NBD model for eco-evolutionary and the extreme case of evolutionary dynamics, both with and without clonal interference.

5.1. No clonal interference

It is assumed that adaptive mutations arise in succession as in Muller's [50] classical model. Here, a resident population can only be invaded by one type of mutant at a time so that there is no interference from other mutations. This means that either the current resident or mutant goes extinct before another mutation arises. This behaviour is obtained in our framework in the rare mutation limit, $\mu(i) \rightarrow 0 \forall i$, similar to Champagnat et al. [6] who derive adaptive dynamics [45, 12] in this limit. However, we could also consider no mutation, $\mu(i) = 0 \forall i$, which is consistent with evolutionary graph theory [2]. We assume no mutation as the results are identical for the evolutionary scenario considered.

We consider an evolutionary scenario that plays out between two types; resident (trait 0) and mutant (trait 1), so $\mathcal{U} = \{0, 1\}$. A mutant is introduced into a resident population by replacing a resident selected uniformly at random, and the individuals then compete with each other. In the limit of infinite time, the population will go to extinction since this is the only true absorbing state.

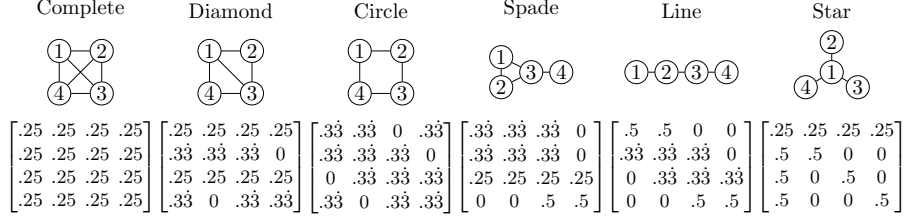


Figure 1: 4-node networks where all outgoing edges from a site with k neighbours are weighted $1/(k+1)$ including self-loops.

However, before this the population must reach a state where only one type remains. We are interested in the hitting probability for the set of states where only the mutant type remains, since this provides a measure of how successful the mutant type is.

The probability of reaching a state with only the mutant type is formally defined in our framework as follows. Let $\mathcal{R} = \{\mathcal{I} : U_i = 0 \forall i \in \mathcal{I}\}$ be the set of states where only the resident type remains; i.e. there is at least one resident but no mutants. Similarly, let $\mathcal{M} = \{\mathcal{I} : U_i = 1 \forall i \in \mathcal{I}\}$ be the set of states where only the mutant type remains. We want the probability of hitting \mathcal{M} from an initial population state \mathcal{I} . This probability, denoted $\rho(\mathcal{I})$, is calculated by solving the equation

$$\begin{cases} \mathcal{L}_c \rho(\mathcal{I}) = 0 & \mathcal{I} \notin \mathcal{M} \cup \mathcal{R}, \\ \rho(\mathcal{I}) = 0 & \mathcal{I} \in \mathcal{R}, \\ \rho(\mathcal{I}) = 1 & \mathcal{I} \in \mathcal{M}. \end{cases} \quad (12)$$

The first line says the population is in a state with both mutants and residents so the infinitesimal generator for modified dynamics, \mathcal{L}_c , is used to specify how the hitting probability changes with an infinitesimally small change in time. Recall that c is used to control the strength of the negative ecological feedback loop. The second line says the hitting probability is 0 as the population cannot hit a state with only mutants starting from a state with only residents. The third line says the hitting probability is 1 as the population is already in a state with only mutants.

Since there is no mutation, a mutant is assumed to be equally likely to appear on any given site. We will therefore consider an initial state with 1 mutant and $N-1$ residents where each site is occupied by one individual only. This allows us to make comparisons with evolutionary graph theory where these are the only possible initial states. The average of ρ for an initial mutant placed uniformly at random is given by

$$\bar{\rho} = \frac{1}{N} \sum_{n=1}^N \rho(\{\mathcal{I}_0 \setminus \{(0, n)\}\} \cup \{(1, n)\}), \quad (13)$$

where $\mathcal{I}_0 = \{(0, 1), (0, 2), \dots, (0, N)\}$ is the state with one resident on each site.

This can be used to compare different NBD dynamics when mutants are assumed to have identical death rates to the residents ($\delta_0 = \delta_1$ and $\gamma_{u,v} =$

$\gamma_{v,u} \forall u, v \in \{0, 1\}$) but an advantageous birth rate ($\beta_1 > \beta_0$). The following cases are considered:

1. SIS dynamics ($\delta_0 = \delta_1 > 0$ and $s = 0$).
2. SIS dynamics with invasion ($\delta_0 = \delta_1 > 0$ and $s = 1$).
3. SIS dynamics with invasion and no natural death ($\delta_0 = \delta_1 = 0$ and $s = 1$).

In Figure 2, $\bar{\rho}$ is plotted against the negative feedback amplifier c for the networks shown in Figure 1. It is observed that

$$\bar{\rho}^{(i)} < \bar{\rho}^{(ii)} < \bar{\rho}^{(iii)} \quad (14)$$

for all networks where $\bar{\rho}^{(i)}$, $\bar{\rho}^{(ii)}$ and $\bar{\rho}^{(iii)}$ are values of $\bar{\rho}$ in cases (i), (ii) and (iii) respectively. SIS-type dynamics are therefore the least beneficial for the spread of an advantageous mutant. Moving from (i) to (ii), shows that allowing invasion is beneficial, since $\bar{\rho}$ shifts up with the networks maintaining their order. As we move from (ii) to (iii), disallowing natural death provides a further benefit, since $\bar{\rho}$ shifts higher up. However, the networks now change their order. In particular, the combined effect of allowing invasion and disallowing natural death is largest in the star network and smallest in the complete network.

To investigate the difference between the complete and star networks, we analytically calculate $\bar{\rho}$ for NBD evolutionary dynamics ($c \rightarrow \infty$). In this case the population cannot go extinct and therefore fixates in \mathcal{M} or \mathcal{R} , i.e. indefinitely remains in a state where there is only one type. Therefore, $\bar{\rho}$ is called the average fixation probability of mutants, a quantity widely studied in population evolution [56].

5.1.1. Average hitting probability for a complete network with NBD evolutionary dynamics

Consider a complete network with arbitrary weights

$$W_{i,j} = w > 0 \quad \forall i, j \in \{1, \dots, N\}. \quad (15)$$

The average fixation probability of a single initial mutant in this network is given by the formula of Karlin and Taylor [34]

$$\bar{\rho}_{\text{comp}} = \left(1 + \sum_{j=1}^{N-1} \prod_{k=1}^j r_k \right)^{-1} \quad (16)$$

where r_k for NBD evolutionary dynamics is given by

$$r_k = \frac{s\beta_0 w \frac{(\delta_1 + \gamma_{1,0})}{(\delta_0 + \delta_1 + \gamma_{0,1} + \gamma_{1,0})} + \delta_1 \frac{\beta_0}{(N-k)\beta_0 + (k-1)\beta_1}}{s\beta_1 w \frac{(\delta_0 + \gamma_{0,1})}{(\delta_0 + \delta_1 + \gamma_{0,1} + \gamma_{1,0})} + \delta_0 \frac{\beta_1}{(N-k-1)\beta_0 + k\beta_1}}. \quad (17)$$

The term r_k is the backward bias of mutants or forward bias of residents. It is obtained by dividing the rate of a resident increasing by the rate of a mutant increasing in a state where there are k mutants (and $N - k$ residents). Details given in Appendix E.

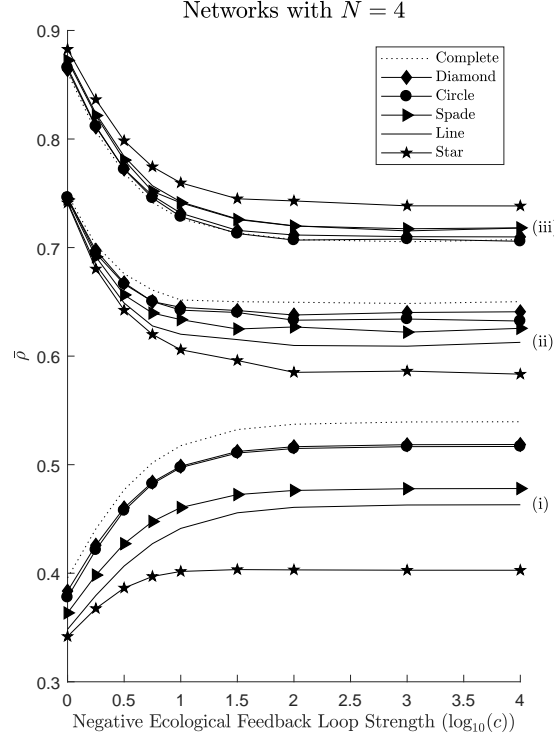


Figure 2: $\bar{\rho}$ in the networks given in Figure 1 for the three different cases considered, they are labelled (i)-(iii) on the right-hand side. For all cases, we set $\beta_0 = 3$, $\beta_1 = 10$, and $\gamma_{u,v} = 5 \forall u, v \in \{0, 1\}$. For cases (i) and (ii) we have $\delta_u = 1$. In case (i), $\bar{\rho}$ is calculated by analytically solving equation (12), for details on how to do this using a state transition matrix see Hindersin and Traulsen [29]. In cases (ii) and (iii), $\bar{\rho}$ are calculated by running 10^5 simulations (see Appendix I for details).

Table 3 shows the bias and average fixation probability for the three cases we consider. The probabilities shown are a closed-form version of equation (16) such that: (i) is obtained from Hindersin and Traulsen [29]; (ii) is not shown as there is no simple analytical form; (iii) is obtained from the Moran probability [48] as the bias is constant. Analysis of the biases in Table 3 reveals

$$r_k^{(i)} > r_k^{(ii)} > r_k^{(iii)}, \quad (18)$$

where $r_k^{(i)}, r_k^{(ii)}, r_k^{(iii)}$ is r_k in cases (i), (ii), (iii) respectively. The proof is given in Appendix F. The key requirement for equation (18) to hold is $\beta_1 > \beta_0$, which we assume is true. Equation (18) implies that equation (14) holds for all $N > 1$ because, as seen in equation (16), a larger bias gives a lower fixation probability. The difference between these cases diminishes as $N \rightarrow \infty$ because their biases all converge to β_0/β_1 , this is seen in Table 3 where $\lim_{N \rightarrow \infty} r_k = \beta_0/\beta_1 \forall k$ in all cases.

Figure 3 shows $\bar{\rho}$ (equation 13) plotted against c in the complete network. Numerically, we observe that $\bar{\rho}$ converges to $\bar{\rho}_{\text{comp}}$ as c gets large, showing that the negative ecological feedback loop functions as desired.

Table 3: Bias and average fixation probability in complete network for NBD evolutionary dynamics. Cases considered assume an advantageous mutant with $\beta_1 > \beta_0$.

Case/ EGT Dynamics	Bias (r_k , $k = 1, \dots, N - 1$)	Avg. Fixation Prob. ($\bar{\rho}_{\text{comp}}$)
(i) SIS-type dynamics ($\delta_0 = \delta_1 > 0$, $s = 0$)/ dB	$\frac{\beta_0}{\beta_1} \frac{k\beta_1 + (N - k - 1)\beta_0}{(N - k)\beta_0 + (k - 1)\beta_1}$	$\frac{N - k}{N} \frac{1 - (\beta_0/\beta_1)}{1 - (\beta_0/\beta_1)^{N-1}}$
(ii) then allow invasion ($\delta_0 = \delta_1 = \delta > 0$, $s = 1$)/ None	$\frac{s\beta_0 w \frac{1}{2} + \delta \frac{\beta_0}{(N-k)\beta_0 + (k-1)\beta_1}}{s\beta_1 w \frac{1}{2} + \delta \frac{\beta_1}{(N-k-1)\beta_0 + k\beta_1}}$	No simple analytical form.
(iii) then disallow natural death ($\delta_0 = \delta_1 = 0$, $s =$ 1)/ LB, Bd	β_0/β_1	$\frac{1 - (\beta_0/\beta_1)}{1 - (\beta_0/\beta_1)^N}$

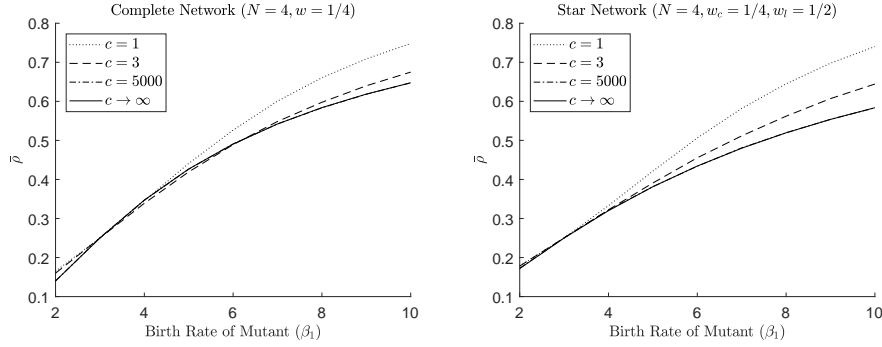


Figure 3: $\bar{\rho}$ plotted against the birth rate of a mutant (β_1) in the complete and star networks when using NBD dynamics with $\beta_0 = 3$, $\delta_u = 1$ and $\gamma_{u,v} = 5 \forall u, v \in \{0, 1\}$. For $c \rightarrow \infty$, $\bar{\rho}$ is given by $\bar{\rho}_{\text{comp}}$ for the complete network and $\bar{\rho}_{\text{star}}$ for the star network. For other values of c , $\bar{\rho}$ is calculated by running 10^6 simulations (see Appendix I for details). As c gets larger we can see that $\bar{\rho}$ converges to $\bar{\rho}_{\text{comp}}$ for the complete network and $\bar{\rho}_{\text{star}}$ for the star network. In particular, the plots for $c = 5000$ and $c \rightarrow \infty$ overlap with one another.

5.1.2. Average hitting probability for a star network with NBD evolutionary dynamics

Consider the star network with weights

$$W_{i,j} = \begin{cases} w_c > 0 & i = 1 \text{ and } j = 1, 2, \dots, N, \\ w_l > 0 & i = 2, 3, \dots, N \text{ and } j = 1, \\ 0 & \text{otherwise.} \end{cases} \quad (19)$$

Site 1 is called the centre site as it is connected to all other $N - 1$ sites called the leaves, which are only connected to the centre. The average fixation probability in this network, denoted $\bar{\rho}_{\text{star}}$, is given by the formula of Hadjichrysanthou et al. [25], see Appendix G for details. For the three cases considered, it can be shown that equation (14) holds when $N \rightarrow \infty$, see Appendix H for details. Note that for the complete network we were able to show this for all N .

Let there be k mutants ($N - 1 - k$ residents) on leaf sites. A mutant in the centre replaces a resident on a leaf with rate

$$(N - 1 - k) \left(sw_c \beta_1 \frac{\delta_0 + \gamma_{0,1}}{\delta_0 + \delta_1 + \gamma_{0,1} + \gamma_{1,0}} + \delta_0 \right), \quad (20)$$

whereas a resident in the centre is replaced by a mutant on a leaf with rate

$$k \left(sw_l \beta_1 \frac{\delta_0 + \gamma_{0,1}}{\delta_0 + \delta_1 + \gamma_{0,1} + \gamma_{1,0}} + \delta_0 \frac{\beta_1}{(N - 1 - k)\beta_0 + k\beta_1} \right). \quad (21)$$

For more information on these rates see Appendix G. We use these equations to investigate the interplay between the BD and DB components of the NBD evolutionary dynamics. In particular, consider the case where $w_c = 1/N$ and $w_l = 1/2$ so that the birth rate is exactly $\beta_u \forall u \in \{0, 1\}$. As N gets larger, the BD component in equation (20) and the DB component in equation (21) get smaller. This means that the highly connected centre individual is more reliant on DB to spread its offspring whereas the less connected leaf individuals are more reliant on BD to spread their offspring.

Figure 3 shows $\bar{\rho}$ (equation 13) for different values of c in the star network. Its qualitative properties are similar to that of the complete network and we once again see that the negative ecological feedback loop functions as desired.

5.1.3. Comparison of average hitting probabilities for complete and star networks

Lieberman et al. [40] show that when using Bd dynamics, the star network amplifies the average fixation probability when compared to the complete network, i.e. $\bar{\rho}_{\text{star}} > \bar{\rho}_{\text{comp}}$. By using NBD evolutionary dynamics we can gain further insight as to why this is the case.

In source-sink metapopulation dynamics [57], a source is a site that is a net exporter of individuals whereas a sink is a site that is a net importer of individuals. A source site is advantageous in comparison to a sink site as more offspring are produced. In the star network, to check whether a leaf or the centre site behaves as a source we set $\beta_u = \beta$, $\delta_u = \delta$ and $\gamma_{u,v} = \gamma \forall u, v \in \{0, 1\}$, i.e. both residents and mutants are neutral. In case (iii) we then have that, from equation (20), the rate at which an offspring born in the centre replaces a leaf individual is

$$w_c \beta \frac{1}{2},$$

whereas, from equation (21), the rate at which an offspring born on a leaf replaces the centre individual is

$$w_l \beta \frac{1}{2}.$$

A leaf site is therefore a source when $w_l > w_c$ and sink when $w_l < w_c$. When calculating $\bar{\rho}_{\text{star}}$ a randomly placed initial mutant is more likely to appear on a leaf. An advantageous mutant is therefore likely to do better when leaf sites are sources. In particular, when Bd dynamics is in operation leaf sites are sources as $w_c = 1/N$ and $w_l = 1/2$ so the star network amplifies the average

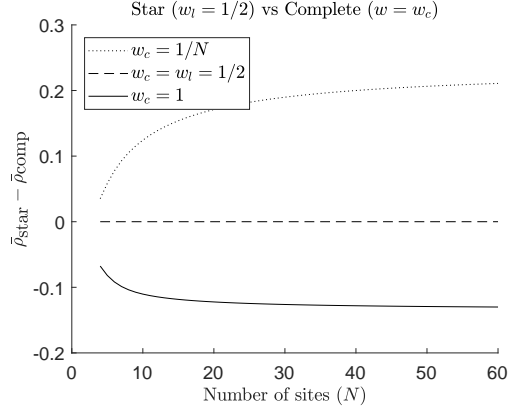


Figure 4: Plot of $\bar{\rho}_{\text{star}} - \bar{\rho}_{\text{comp}}$ against the number of sites (N) when using NBD evolutionary dynamics with $\beta_0 = 3$, $\beta_1 = 8$, $\gamma_{u,v} = 5$ and $\delta_u = 0 \forall u, v \in \{0, 1\}$. It shows that the star network is no longer an amplifier when $w_c > w_l$.

fixation probability of an advantageous mutant. This is verified in figure 4 which illustrates that $\bar{\rho}_{\text{star}} > \bar{\rho}_{\text{comp}}$ when $w_l > w_c$, $\bar{\rho}_{\text{star}} < \bar{\rho}_{\text{comp}}$ when $w_l < w_c$, and $w_l = w_c$ is the boundary between amplification and suppression where $\bar{\rho}_{\text{star}} = \bar{\rho}_{\text{comp}}$.

The natural death rate plays a fundamental role since it can prevent a leaf site from being a source. This is seen in case (ii) when comparing the centre site to a leaf site when both residents and mutants are neutral. That is, from equation (20), the rate at which an offspring born in the centre replaces a leaf individual is

$$w_c \beta \frac{1}{2} + \delta,$$

whereas, from equation (21), the rate at which an offspring born on a leaf replaces the centre individual is

$$w_l \beta \frac{1}{2} + \frac{\delta}{N}.$$

The natural death rate can therefore prevent a leaf site from being a source when $w_l > w_c$. In particular, a leaf individual has to compete with other leaf individuals to place its offspring in the centre when the centre individual dies but this is not the case for the centre individual when a leaf individual dies. Another way to look at this is that a natural death rate limits the amount of time a leaf individual has to spread its offspring before it dies. The natural death rate can therefore suppress the fixation probability of an advantageous mutant in the star network. This is verified in figure 5, where increasing the death rate causes $\bar{\rho}_{\text{star}} - \bar{\rho}_{\text{comp}}$ to decrease, such that the star network is no longer an amplifier of selection. This is consistent with Hadjichrysanthou et al. [25] which shows that the star is not an amplifier under Db and dB dynamics.

5.2. With clonal interference

Here we no longer assume that adaptations are successive, and instead take into account the effect of clonal interference, which has been demonstrated in a

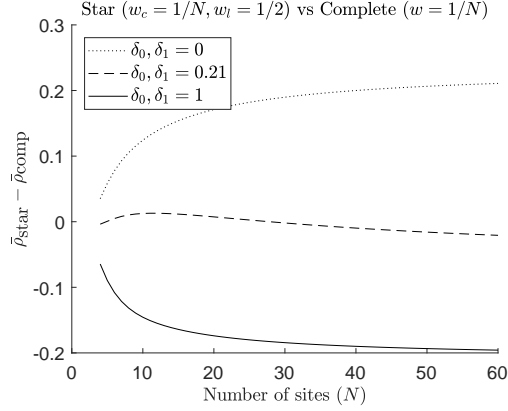


Figure 5: Plot of $\bar{\rho}_{\text{star}} - \bar{\rho}_{\text{comp}}$ against the number of sites (N) when using NBD evolutionary dynamics with $\beta_0 = 3$, $\beta_1 = 8$, $\gamma_{u,v} = 5$ and $\delta_u = 0, 0.21, 1 \forall u, v \in \{0, 1\}$. It shows that the star network is no longer an amplifier as the natural death rate increases.

range of asexual organisms [33]. For clonal interference in unstructured populations, it has been shown that the fixation probability of a beneficial mutation decreases as the population size and mutation rate increases [20]. The inclusion of clonal interference will therefore provide a better understanding of the impact that population structure has on the success of an adaptive mutation.

To study the effect of clonal interference we consider the evolutionary scenario considered in Gerrish & Lenski [20]. Here, a resident population (type 0) can be invaded by two kinds of mutant, an original mutant (type 1) and a superior mutant (type 2), i.e. $\mathcal{U} = \{0, 1, 2\}$. The population initially consists of the resident and original mutant types such that, to be consistent with the no clonal interference case, an original mutant is introduced into a resident population by randomly replacing a resident. A superior mutant is introduced later into the population through random mutation in the resident type. Therefore, there is initially competition between the resident and original mutant types, but the superior mutant type can interfere. We are interested in the probability of reaching a state where only the original mutant type remains since it is a measure of its success in the presence of clonal interference.

To define this formally, we assume that a resident has constant mutation probability and that its mutated offspring is a superior mutant, i.e. $\mu(i) = \mu$ if $U_i = 0$ but $\mu(i) = 0$ otherwise, and $M(u, v) = 1$ if $u = 0, v = 2$ but $M(u, v) = 0$ otherwise. Note that the integral in equation (1) is changed to a summation because of the discrete number of mutations. Let \mathcal{R} be the set of states where only the resident type remains as we previously defined, and \mathcal{M}_1 and \mathcal{M}_2 be the set of states with all type 1 and type 2 individuals respectively. We want to calculate the probability, ψ , of hitting \mathcal{M}_1 conditional on not hitting $\mathcal{R} \cup \mathcal{M}_2$ starting from an initial state \mathcal{I} . When using the modified dynamics, this is found by solving the equation

$$\begin{cases} \mathcal{L}_c \psi(\mathcal{I}) = 0 & \mathcal{I} = \{(u, x) \notin \mathcal{M}_1 : \exists u = 1\} \\ \psi(\mathcal{I}) = 0 & \mathcal{I} \in \mathcal{R} \cup \mathcal{M}_2, \\ \psi(\mathcal{I}) = 1 & \mathcal{I} \in \mathcal{M}_1. \end{cases} \quad (22)$$

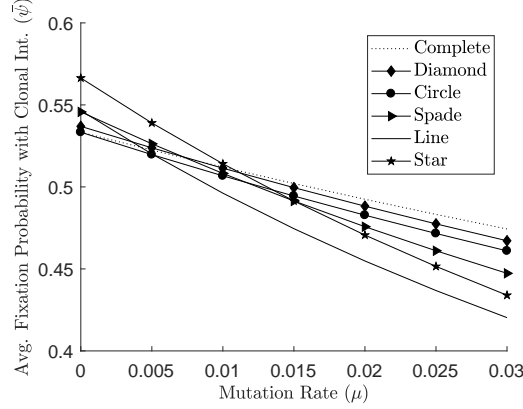


Figure 6: Comparison of average fixation probability with clonal interference ($\bar{\psi}$) when using NBD evolutionary dynamics. The parameters are set as follows $\beta_0 = 1$, $\beta_1 = 2$, $\beta_2 = 3$, $\delta_u = 0$, $\gamma_{u,v} = 1$ for all $u, v \in \{0, 1, 2\}$. $\bar{\psi}$ is calculated by analytically solving equation (22) using a state transition matrix [29].

We consider the initial states with 1 original mutant and $N - 1$ residents where each site is occupied by one individual only, so the average of ψ for a randomly placed initial original mutant is

$$\bar{\psi} = \frac{1}{N} \sum_{i \in \mathcal{I}_0} \psi(\{\mathcal{I}_0 \setminus \{i\}\} \cup \{(1, X_i)\}).$$

Note that when $\mu = 0$, there is no clonal interference and we have that $\psi = \rho$ (so $\bar{\psi} = \bar{\rho}$).

Clonal interference reduces the amount of time that a mutant of type 1 has to fixate, since the longer it takes the more likely a mutant of type 2 will appear. Without clonal interference, the complete network has the lowest fixation time whereas, for example, the star network is substantially higher [18, 62, 46]. We should therefore expect the complete network to be least affected as the mutation rate increases in comparison to the star and other networks. To show that this is indeed the case, we plot $\bar{\psi}$ for different mutation rates in figure 6 for the networks with four sites given in figure 1 when using NBD evolutionary dynamics ($c \rightarrow \infty$). The population does not go extinct in this case and fixates in either \mathcal{M}_1 or \mathcal{M}_2 , so $\bar{\psi}$ is the average fixation probability of an original mutant with clonal interference. The average fixation probability under clonal interference decreases in all networks, with the complete network being the least affected since it has the lowest fixation time.

The circulation theorem [41, 40] in evolutionary graph theory identifies networks whose fixation probability is equal to the Moran probability. This theorem holds for simple evolutionary dynamics [55], and generally fails for other dynamics. Here we see it failing due to clonal interference. In figure 1, we see that the fixation probability is identical for complete and circle networks because the circulation theorem holds, but this is no longer the case when $\mu > 0$.

6. Discussion

We have constructed a model for evolution in network-structured populations which is based on individual-level ecological processes and which allows the population size, density and composition to change. This represents an advance on current evolutionary graph theory models which only allow the composition of the population to change. In sections 3 and 4 we showed, using a negative ecological feedback loop, that suppression of ecological dynamics in our framework’s eco-evolutionary dynamics, leaves the pure evolutionary dynamics of evolutionary graph theory. However, this process highlights the extreme assumptions required and the departure from underpinning ecological processes. In particular, fixed population size and density obtained by suppressing ecological dynamics are an exception [44, 10] and can prevent us capturing biological processes accurately.

In section 4 we used our framework to define the network birth and death model (NBD) where the ecological dynamics specify that the carrying capacity is dependent upon the population composition. In particular, intra-site competition is taken from Huang et al. [32], which provides a way to consider evolutionary games [43]. NBD contains the SIS epidemic model and its variations, such that the birth rate is seen as the infection rate and the death rate as the recovery rate. By suppressing the ecological dynamics in NBD, we also obtained evolutionary graph theory dynamics. This enabled fitness (used in evolutionary graph theory to measure reproductive success) to be related to birth and death rates (Table 2). Depending upon the dynamics, we found that fitness is either proportional to the birth rate or inversely proportional to the death rate. This shows that the method used to derive evolutionary graph theory dynamics from eco-evolutionary dynamics correctly identifies the relationship between fitness and birth and death rates.

In section 5, the NBD model is used to compare the long-term success of a mutant type invading a resident population in different networks. We first considered the case with no clonal interference. When the strength of the negative ecological feedback loop (c) was set to 0, network structure had little effect such that an advantageous mutant had relatively similar levels of success in all the networks considered. Instead, intra-site competition due to offspring being placed on occupied sites played a much more important role. In particular, allowing intra-site competition significantly increased the success of an advantageous mutant, which increased further when natural death was disallowed. As the strength of the negative ecological feedback loop was increased ($c > 0$) the effect of network structure increased. This is because increasing c results in increased competition for a site as the population approaches the equilibrium state with one individual per site much faster. When ecological dynamics are completely suppressed ($c \rightarrow \infty$), and we recover evolutionary graph theory, an invading mutant type either fixates or goes extinct. With Bd dynamics, the star network is known to amplify the fixation probability of an advantageous mutant [40]. We show that this is because Bd dynamics allow sites in the star network to act as sources, i.e. are net exporters of offspring. Since Bd dynamics do not allow individuals to die naturally, we show numerically (Figure 5) that allowing natural death can prevent these sites from being sources and result in the star network suppressing the fixation probability. This suggests that amplification of selection requires dynamics in which source sites can exist.

For all networks considered, the fixation probability of a mutant with clonal interference decreased as the mutation rate increased (Figure 6). This is expected because the higher the mutation rate the more likely it is that another beneficial mutation will appear and interfere with the initial mutant fixating. The effect of clonal interference on fixation was lower for more homogeneous networks (complete, diamond, circle) than for the networks with some heterogeneity (line, star). This is consistent with Frean et al. [18], which showed that fixation times are longer in the star network than in the complete network, and thus the star network is more susceptible to clonal interference.

To implement eco-evolutionary dynamics on a network-structured population, we combined birth with movement such that offspring can be placed on a different connected site from their parent. This means that the movement is local and dependent upon the network-structure of the population. With the exception of bD dynamics, we were able to recover all other standard evolutionary graph theory dynamics. This shows that the localised movement in standard evolutionary graph theory dynamics is primarily based on this mechanism where movement is combined with birth, but also highlights that other options exist. In the case of bD dynamics, movement would need to be separated from birth because it requires an offspring to be initially placed in the same site as its parent before moving to another site. Using our framework as a skeleton, we can implement this by adding an additional term to the infinitesimal dynamics that accounts for a change in state caused by the movement of individuals. However, this movement term would require restrictions so that individuals can move only once to a neighbouring site, highlighting a further unrealistic assumption required to obtain evolutionary graph theory dynamics.

Appendix A. Generator Details

Here we provide details on the generator and hitting probability given in section 2. Though not in the main text, details of the hitting time are also provided.

The infinitesimal generator describes how the expected values of functions of our model change in infinitesimal time intervals. For a function f acting on the stochastic process $\Sigma(t)$, the infinitesimal generator, \mathcal{L} , is defined as [54]

$$\mathcal{L}f(y) = \frac{d}{dt}\mathbb{E}[f(\Sigma(t))]|_{t=0} = \lim_{t \rightarrow 0} \frac{\mathbb{E}[f(\Sigma(t))] - f(y)}{t}.$$

Appendix A.1. Hitting Probability

The hitting probability of a state $A \in S$ is the probability that the Markov process eventually reaches state A , given that it started in some state i . Let T^A be the time when the Markov process first enters state A , then the hitting probability from an initial state i is given by

$$h_A(i) = P(T^A < \infty | \Sigma(0) = i).$$

Using the infinitesimal generator, we can find equations describing the hitting probability. From the definition of the generator, we have

$$\mathcal{L}h_A(i) = \frac{d}{dt}\mathbb{E}[h_A(\Sigma(t)) | \Sigma(0) = i].$$

Given that the Markov process starts in state i , the expected value of the hitting probability does not change with time, and therefore this derivative must be equal to zero, giving

$$\mathcal{L}h_A(i) = 0.$$

If our initial state $i = A$, then the hitting probability is equal to 1, so we have $h_A(A) = 1$. In summary, the hitting probability is given by solving

$$\begin{cases} \mathcal{L}h_A(i) = 0, \\ h_A(A) = 1. \end{cases} \quad (\text{A.1})$$

Appendix A.2. Hitting Time

The expected time until the Markov process reaches a state A from an initial state i , is defined as

$$k_A(i) = \mathbb{E}[T^A | \Sigma(0) = i].$$

From the definition of the generator, we have

$$\mathcal{L}k_A(i) = \frac{d}{dt} \mathbb{E}[k_A(\Sigma(t)) | \Sigma(0) = i].$$

The derivative can be calculated by

$$\frac{d}{dt} \mathbb{E}[k_A(\Sigma(t)) | \Sigma(0) = i] = \lim_{h \rightarrow 0} \frac{\mathbb{E}[k_A(\Sigma(t+h)) | \Sigma(0) = i] - \mathbb{E}[k_A(\Sigma(t)) | \Sigma(0) = i]}{h}$$

Since both of the expectations on the right-hand side condition on $\Sigma(0) = i$, the expected hitting time from 0 must be equal. The expected time from $t+h$ therefore has to be h less than the expected time from t , so this becomes

$$\frac{d}{dt} \mathbb{E}[k_A(\Sigma(t)) | \Sigma(0) = i] = \lim_{h \rightarrow 0} \frac{-h}{h} = -1.$$

Therefore, it must hold that

$$\mathcal{L}k_A(i) = -1.$$

If our initial state $i = A$, then the expected hitting time is equal to 0, so we have $k_A(A) = 0$. To summarise, the expected hitting time is given by solving

$$\begin{cases} \mathcal{L}k_A(i) = -1, \\ k_A(A) = 0. \end{cases} \quad (\text{A.2})$$

Appendix B. Hitting probability for modified dynamics

Here we show how the hitting probability for modified dynamics, equation (5), is obtained. We have that

$$\begin{aligned} 0 &= \lim_{c \rightarrow \infty} \mathcal{L}_c h_A(\mathcal{I}) \\ 0 &= \lim_{c \rightarrow \infty} \sum_{i \in \mathcal{I}} \sum_{x \in \mathcal{X}} [1 - \mu(i)] B(c, i, x, \mathcal{I}) [h_A(\mathcal{I} \cup \{(U_i, x)\}) - h_A(\mathcal{I})] \end{aligned}$$

$$\begin{aligned}
& + \sum_{i \in \mathcal{I}} \sum_{x \in \mathcal{X}} \mu(u) B(c, i, x, \mathcal{I}) \int_{\mathbb{R}^l} [h_{\mathcal{A}}(\mathcal{I} \cup \{(w, x)\}) - h_{\mathcal{A}}(\mathcal{I})] M(U_i, w) dw \\
& + \sum_{i \in \mathcal{I}} D(c, i, \mathcal{I}) [h_{\mathcal{A}}(\mathcal{I} \setminus \{i\}) - h_{\mathcal{A}}(\mathcal{I})].
\end{aligned}$$

Let

$$\lambda_{\mathcal{I}} = \lim_{c \rightarrow \infty} \sum_{i \in \mathcal{I}} \sum_{x \in \mathcal{X}} B(c, i, x, \mathcal{I}) + D(c, i, \mathcal{I}).$$

then rearranging gives

$$\begin{aligned}
h_{\mathcal{A}}(\mathcal{I}) &= \lim_{c \rightarrow \infty} \frac{1}{\lambda_{\mathcal{I}}} \sum_{i \in \mathcal{I}} \sum_{x \in \mathcal{X}} B(c, i, x, \mathcal{I}) \left([1 - \mu(i)] h_{\mathcal{A}}(\mathcal{I} \cup \{(U_i, x)\}) \right. \\
& \quad \left. + \mu(i) \int_{\mathbb{R}^l} h_{\mathcal{A}}(\mathcal{I} \cup \{(w, x)\}) M(U_i, w) dw \right) \\
& \quad + D(c, i, \mathcal{I}) h_{\mathcal{A}}(\mathcal{I} \setminus \{i\}).
\end{aligned}$$

We assume that the population starts in a state \mathcal{I} where $|\mathcal{I}|_x = 1 \ \forall x \in \mathcal{X}$, we then have that

$$\begin{aligned}
h_{\mathcal{A}}(\mathcal{I}) &= \frac{1}{\lambda_{\mathcal{I}}} \sum_{i \in \mathcal{I}} \sum_{x \in \mathcal{X}} b(i, x, \mathcal{I}) \left([1 - \mu(i)] h_{\mathcal{A}}(\mathcal{I} \cup \{(U_i, x)\}) \right. \\
& \quad \left. + \mu(i) \int_{\mathbb{R}^l} h_{\mathcal{A}}(\mathcal{I} \cup \{(w, x)\}) M(U_i, w) dw \right) \\
& \quad + d(i, \mathcal{I}) h_{\mathcal{A}}(\mathcal{I} \setminus \{i\})
\end{aligned}$$

since all sites have density 1. From state \mathcal{I} we consider the following different states \mathcal{J} that the population can transition to.

1. For $\mathcal{J} = \mathcal{I} \cup \{(u, x)\}$ we have that

$$\begin{aligned}
h_{\mathcal{A}}(\mathcal{J}) &= \lim_{c \rightarrow \infty} \frac{1}{\lambda_{\mathcal{J}}} \sum_{j \in \mathcal{J}} \sum_{y \in \mathcal{X}} [1 - \mu(j)] B(c, j, y, \mathcal{J}) h_{\mathcal{A}}(\mathcal{J} \cup \{j\}) \\
& \quad + \mu(j) B(c, j, y, \mathcal{J}) \int_{\mathbb{R}^l} h_{\mathcal{A}}(\mathcal{J} \cup \{(w, y)\}) M(U_j, w) dw \\
& \quad + D(c, j, \mathcal{J}) h_{\mathcal{A}}(\mathcal{J} \setminus \{j\}).
\end{aligned}$$

The birth rate in this case is given by

$$\lim_{c \rightarrow \infty} B(c, j, y, \mathcal{J}) = \lim_{c \rightarrow \infty} c^{H_0[-|\mathcal{J}_y|]} b(j, y, \mathcal{J}) = b(j, y, \mathcal{J})$$

as $H_0[-|\mathcal{J}_y|] = 0 \ \forall y \in \mathcal{X}$ as there are no empty sites. Similarly, the death in this case is given by

$$\lim_{c \rightarrow \infty} D(c, j, \mathcal{J}) = \lim_{c \rightarrow \infty} c^{H_2[|\mathcal{I}_{x_j}|]} d(j, \mathcal{J}) = \lim_{c \rightarrow \infty} c^{\delta_{x_j, x}} d(j, \mathcal{J})$$

as site x is the only site with two individuals and $\delta_{m, n}$ is the Kronecker delta function. This means that

$$\frac{\lim_{c \rightarrow \infty} B(c, j, y, \mathcal{J})}{\lambda_{\mathcal{J}}} = 0 \quad \forall j \in \mathcal{J}, y \in \mathcal{X}$$

and

$$\frac{\lim_{c \rightarrow \infty} D(c, j, \mathcal{J})}{\lambda_{\mathcal{J}}} = \frac{\lim_{c \rightarrow \infty} c^{\delta_{X_j, x}} d(j, \mathcal{J})}{\sum_{j \in \mathcal{J}} \lim_{c \rightarrow \infty} c^{\delta_{X_j, x}} d(j, \mathcal{J})} = \frac{\delta_{X_j, x} d(j, \mathcal{J})}{\sum_{j \in \mathcal{J}_x} d(j, \mathcal{J})}.$$

The hitting probability from state \mathcal{J} is then given by

$$h_{\mathcal{A}}(\mathcal{J}) = \sum_{j \in \mathcal{J}_x} \frac{d(j, \mathcal{J}) h_{\mathcal{A}}(\mathcal{J} \setminus \{j\})}{\sum_{k \in \mathcal{J}_x} d(k, \mathcal{J})}.$$

2. For $\mathcal{J} = \mathcal{I} \setminus \{i\}$ such that $i \in \mathcal{I}$, by following a similar set of arguments as we have for case 1 we obtain the hitting probability from state \mathcal{J} as follows

$$h_{\mathcal{A}}(\mathcal{J}) = \sum_{j \in \mathcal{J}} \frac{b(j, X_i, \mathcal{J})}{\sum_{j \in \mathcal{J}} b(j, X_i, \mathcal{J})} \left([1 - \mu(j)] h_{\mathcal{A}}(\mathcal{J} \cup \{(U_j, X_i)\}) \right. \\ \left. + \mu(j) \int_{\mathbb{R}^l} h_{\mathcal{A}}(\mathcal{J} \cup \{(w, X_i)\}) M(U_j, w) dw \right).$$

Substituting the hitting probability from \mathcal{J} for these two cases into the hitting probability from \mathcal{I} gives

$$h_{\mathcal{A}}(\mathcal{I}) = \frac{1}{\lambda_{\mathcal{I}}} \sum_{i \in \mathcal{I}} \sum_{x \in \mathcal{X}} b(i, x, \mathcal{I}) \left([1 - \mu(i)] \frac{\sum_{j \in \mathcal{I}_x \cup \{(U_i, x)\}} d(j, \mathcal{I} \cup \{(U_i, x)\}) h_{\mathcal{A}}(\mathcal{I} \cup \{(U_i, x)\} \setminus \{j\})}{\sum_{j \in \mathcal{I}_x \cup \{(U_i, x)\}} d(j, \mathcal{I} \cup \{(U_i, x)\})} \right. \\ \left. + \mu(i) \int_{\mathbb{R}^l} \frac{\sum_{j \in \mathcal{I}_x \cup \{(w, x)\}} d(j, \mathcal{I} \cup \{(w, x)\}) h_{\mathcal{A}}(\mathcal{I} \cup \{(w, x)\} \setminus \{j\})}{\sum_{j \in \mathcal{I}_x \cup \{(w, x)\}} d(j, \mathcal{I} \cup \{(w, x)\})} M(U_i, w) dw \right) \\ + d(i, \mathcal{I}) \sum_{j \in \mathcal{I} \setminus \{i\}} \frac{b(j, X_i, \mathcal{I} \setminus \{i\})}{\sum_{j \in \mathcal{I} \setminus \{i\}} b(j, X_i, \mathcal{I} \setminus \{i\})} \left([1 - \mu(j)] h_{\mathcal{A}}(\mathcal{I} \setminus \{i\} \cup \{(U_j, X_i)\}) \right. \\ \left. + \mu(j) \int_{\mathbb{R}^l} h_{\mathcal{A}}(\mathcal{I} \setminus \{i\} \cup \{(w, X_i)\}) M(U_j, w) dw \right)$$

This can be rewritten as follows

$$h_{\mathcal{A}}(\mathcal{I}) = \frac{1}{\lambda_{\mathcal{I}}} \sum_{i \in \mathcal{I}} \sum_{j \in \mathcal{I}} \left(b(i, X_j, \mathcal{I}) \frac{d(j, \mathcal{J})}{\sum_{k \in \mathcal{J}_{X_j}} d(k, \mathcal{J})} + d(j, \mathcal{I}) \frac{b(i, X_j, \mathcal{I} \setminus \{j\})}{\sum_{k \in \mathcal{I} \setminus \{j\}} b(k, X_i, \mathcal{I} \setminus \{j\})} \right) [1 - \mu(i)] h_{\mathcal{A}}(\mathcal{J} \setminus \{j\}) \\ + \int_{\mathbb{R}^l} \left(b(i, X_j, \mathcal{I}) \frac{d(j, \mathcal{K})}{\sum_{k \in \mathcal{K}_{X_j}} d(k, \mathcal{K})} + d(j, \mathcal{I}) \frac{b(i, X_j, \mathcal{I} \setminus \{j\})}{\sum_{k \in \mathcal{I} \setminus \{j\}} b(k, X_i, \mathcal{I} \setminus \{j\})} \right) \mu(i) h_{\mathcal{A}}(\mathcal{K} \setminus \{j\}) M(U_i, w) dw$$

where $\mathcal{J} = \mathcal{I} \cup \{(U_i, X_j)\}$ and $\mathcal{K} = \mathcal{I} \cup \{(w, X_j)\}$. This can then be further simplified by writing

$$h_{\mathcal{A}}(\mathcal{I}) = \frac{1}{\lambda_{\mathcal{I}}} \sum_{i \in \mathcal{I}} \sum_{j \in \mathcal{I}} r(i, j, U_i, \mathcal{I}) [1 - \mu(i)] h_{\mathcal{A}}(\mathcal{J} \setminus \{j\}) + \int_{\mathbb{R}^l} r(i, j, w, \mathcal{I}) \mu(i) h_{\mathcal{A}}(\mathcal{K} \setminus \{j\}) M(U_i, w) dw \quad (\text{B.1})$$

where $r(i, j, u, \mathcal{I})$ is the rate at which the offspring of individual i replaces j given that the offspring has trait u .

Appendix C. Infinitesimal generator and hitting probability for evolutionary graph theory

Here we provide the definition of the infinitesimal generator used and the hitting probability obtained for evolutionary graph theory mentioned in section 4. The infinitesimal generator for evolutionary graph theory is defined as follows

$$\mathcal{L}^{\text{EGT}} \phi(\mathcal{I}) = \sum_{i \in \mathcal{I}} \sum_{j \in \mathcal{I}} [1 - \mu(i)] R(i, j, U_i, \mathcal{I}) [\phi(\mathcal{I} \cup \{(U_i, X_j)\}) \setminus \{j\}) - \phi(\mathcal{I})] + \mu(i) \int_{\mathbb{R}^l} R(i, j, w, \mathcal{I}) [\phi(\mathcal{I} \cup \{(w, X_j)\}) \setminus \{j\}) - \phi(\mathcal{I})] M(U_i, w) dw \quad (\text{C.1})$$

where R is the replacement rate in evolutionary graph theory dynamics. Note that R is a function of W but has been dropped for brevity. This generator with continuous mutations has not been considered before but it allows direct comparisons between h^{NBD} and h^{EGT} . In particular, solving equation (A.1) with \mathcal{L}^{EGT} gives the hitting probability in evolutionary graph theory,

$$h_{\mathcal{A}}^{\text{EGT}}(\mathcal{I}) = \frac{1}{\lambda_{\mathcal{I}}} \sum_{i \in \mathcal{I}} \sum_{j \in \mathcal{I}} R(i, j, U_i, \mathcal{I}) [1 - \mu(i)] h_{\mathcal{A}}^{\text{EGT}}(\mathcal{I} \cup \{(U_i, X_j)\}) \setminus \{j\}) + \int_{\mathbb{R}^l} R(i, j, w, \mathcal{I}) \mu(i) h_{\mathcal{A}}^{\text{EGT}}(\mathcal{I} \cup \{(w, X_j)\}) \setminus \{j\}) M(U_i, w) dw, \quad (\text{C.2})$$

where $\lambda_{\mathcal{I}}$ is the rate of leaving state \mathcal{I} . Note that its form is similar that of h^{NBD} .

Appendix D. Deriving standard evolutionary graph theory dynamics

Here we show how we derive standard evolutionary graph theory dynamics from NBD evolutionary dynamics, see section 4.

We need to show that

$$h_{\mathcal{A}}^{\text{NBD}}(\mathcal{I}) = h_{\mathcal{A}}^{\text{EGT}}(\mathcal{I}).$$

We start by observing that for all the standard evolutionary graph theory dynamics, the replacement rate satisfies

$$R(i, j, u, \mathcal{I}) = R(i, j, v, \mathcal{I}) \quad \forall u, v \in \mathcal{U} \quad (\text{D.1})$$

and therefore

$$\begin{aligned}\lambda_{\mathcal{I}} &= \sum_{i \in \mathcal{I}} \sum_{j \in \mathcal{I}} R(i, j, U_i, \mathcal{I}) [1 - \mu(i)] + \int_{\mathbb{R}^l} R(i, j, w, \mathcal{I}) \mu(i) M(U_i, w) dw \\ &= \sum_{i \in \mathcal{I}} \sum_{j \in \mathcal{I}} R(i, j, \mathcal{I}),\end{aligned}$$

where $R(i, j, \mathcal{I})$ is the replacement rate with the type of the offspring dropped. Furthermore, for all the standard evolutionary graph theory dynamics the following also holds

$$\lambda_{\mathcal{I}} = \sum_{i \in \mathcal{I}} \sum_{j \in \mathcal{I}} R(i, j, \mathcal{I}) = 1$$

since the replacement rates are defined as probabilities. We then require that the replacement rate r for NBD evolutionary dynamics have the same property as in equation (D.1), that is,

$$r(i, j, u, \mathcal{I}) = r(i, j, v, \mathcal{I}) \quad \forall u, v \in \mathcal{U}, \quad (\text{D.2})$$

we can therefore use $r(i, j, \mathcal{I})$ as the offspring type can be dropped, and

$$R(i, j, \mathcal{I}) = \frac{r(i, j, \mathcal{I})}{\sum_{n \in \mathcal{I}} \sum_{k \in \mathcal{I}} r(n, k, \mathcal{I})}.$$

This ensures that the hitting probability is identical for both types of dynamics. Recall that the replacement rate for NBD evolutionary dynamics is given by

$$r(i, j, u, \mathcal{I}) = s\beta_{U_i} W_{X_i, X_j} \frac{\delta_{U_j} + \gamma_{U_j, u}}{\delta_{U_j} + \gamma_{U_j, u} + \delta_u + \gamma_{u, U_j}} + \delta_{U_j} \frac{\beta_{U_i} W_{X_i, X_j}}{\sum_{k \in \mathcal{I} \setminus \{j\}} \beta_{U_k} W_{X_k, X_j}}.$$

We can now consider which of the standard evolutionary graph theory dynamics we can obtain from these dynamics.

LB dynamics. Setting $\delta_u = 0$ and $\gamma_{u, v} = \gamma_{v, u} \quad \forall u, v \in \mathcal{U}$ satisfies equation (D.2) and gives

$$\frac{r(i, j, \mathcal{I})}{\sum_{n \in \mathcal{I}} \sum_{k \in \mathcal{I}} r(n, k, \mathcal{I})} = \frac{\beta_{U_i} W_{X_i, X_j}}{\sum_{n \in \mathcal{I}} \sum_{k \in \mathcal{I}} \beta_{U_n} W_{X_n, X_k}}$$

which is identical to the LB dynamics when $\beta_u = F_u \quad \forall u \in \mathcal{U}$.

Bd dynamics. Doing the same as with the derivation of LB dynamics, but setting $W\mathbf{1} = \mathbf{1}$ gives

$$\frac{r(i, j, \mathcal{I})}{\sum_{n \in \mathcal{I}} \sum_{k \in \mathcal{I}} r(n, k, \mathcal{I})} = \frac{\beta_{U_i}}{\sum_{n \in \mathcal{I}} \beta_{U_n}} W_{X_i, X_j}$$

which is identical to the Bd dynamics when $\beta_u = F_u \quad \forall u \in \mathcal{U}$.

Db dynamics. Setting $s = 0$ and $\beta_u = \beta_v \forall u, v \in \mathcal{U}$ satisfies equation (D.2) and gives

$$\frac{r(i, j, \mathcal{I})}{\sum_{n \in \mathcal{I}} \sum_{k \in \mathcal{I}} r(n, k, \mathcal{I})} = \frac{\delta_{U_j} \frac{W_{X_i, X_j}}{\sum_{k \in \mathcal{I} \setminus \{j\}} W_{X_k, X_j}}}{\sum_{n \in \mathcal{I}} \sum_{k \in \mathcal{I} \setminus \{n\}} \delta_{U_n} \frac{W_{X_k, X_n}}{\sum_{m \in \mathcal{I} \setminus \{n\}} W_{X_m, X_n}}} = \frac{\delta_{U_j}}{\sum_{n \in \mathcal{I}} \delta_{U_n}} \frac{W_{X_i, X_j}}{\sum_{k \in \mathcal{I} \setminus \{j\}} W_{X_k, X_j}}$$

which is identical to Db dynamics when $\delta_u = 1/F_u \forall u \in \mathcal{U}$.

dB Dynamics. Setting $s = 0$ and $\delta_u = \delta_v \forall u, v \in \mathcal{U}$ satisfies equation (D.2) and gives

$$\frac{r(i, j, \mathcal{I})}{\sum_{n \in \mathcal{I}} \sum_{k \in \mathcal{I}} r(n, k, \mathcal{I})} = \frac{\delta_{U_j} \frac{\beta_{U_i} W_{X_i, X_j}}{\sum_{k \in \mathcal{I} \setminus \{j\}} \beta_{U_k} W_{X_k, X_j}}}{\sum_{n \in \mathcal{I}} \sum_{k \in \mathcal{I} \setminus \{n\}} \delta_{U_n} \frac{\beta_{U_k} W_{X_k, X_n}}{\sum_{m \in \mathcal{I} \setminus \{n\}} \beta_{U_m} W_{X_m, X_n}}} = \frac{1}{N} \frac{\beta_{U_i} W_{X_i, X_j}}{\sum_{k \in \mathcal{I} \setminus \{j\}} \beta_{U_k} W_{X_k, X_j}}$$

which is identical to dB dynamics when $\beta_u = F_u \forall u \in \mathcal{U}$.

LD Dynamics. These require the competition rate $\gamma_{u,v}$ and therefore (D.2) cannot be satisfied. However, we can bypass this condition by assuming there is no mutation and that there are only two types, i.e. $|\mathcal{U}| = 2$. Note that excluding transitions to the same state will not affect h_A so if we discount transitions to the same state, we would require that

$$\frac{R(i, j, \mathcal{I})}{\sum_{n \in \mathcal{I}} \sum_{\substack{k \in \mathcal{I} \\ U_k \neq U_n}} R(n, k, \mathcal{I})} = \frac{r(i, j, \mathcal{I})}{\sum_{n \in \mathcal{I}} \sum_{\substack{k \in \mathcal{I} \\ U_k \neq U_n}} r(n, k, \mathcal{I})} \quad \text{for } U_j \neq U_i. \quad (\text{D.3})$$

Setting $\delta_u = 0$ and $\beta_u = \beta_v \forall u \in \mathcal{U}$ simplifies the RHS of equation (D.3) to

$$\frac{W_{X_i, X_j} \frac{\gamma_{U_j, U_i}}{\gamma_{U_j, U_i} + \gamma_{U_i, U_j}}}{\sum_{n \in \mathcal{I}} \sum_{\substack{k \in \mathcal{I} \\ U_k \neq U_n}} W_{X_n, X_k} \frac{\gamma_{U_k, U_n}}{\gamma_{U_k, U_n} + \gamma_{U_n, U_k}}} = \frac{W_{X_i, X_j} \gamma_{U_j, U_i}}{\sum_{n \in \mathcal{I}} \sum_{\substack{k \in \mathcal{I} \\ U_k \neq U_n}} W_{X_n, X_k} \gamma_{U_k, U_n}}$$

which for $\gamma_{u,v} = 1/F_u$ when $u \neq v \forall u, v \in \mathcal{U}$ is equivalent to the LHS of equation (D.3) when using LD dynamics.

Appendix E. Derivation of bias (r_k) in complete network for NBD evolutionary dynamics

Here we show how the bias given in equation (17) is obtained. We start by defining the replacement rate in the complete network. For evolutionary

dynamics, we only need to consider population states with one individual on each site. The position of residents and mutants does not matter in these states due to site homogeneity. Therefore, states with the same number of mutants k (which means there are $N - k$ residents) are lumped together and referred to by this number. We are interested in the rate at which the system transitions from some state k to a state with an additional type u individual; i.e. with $k - (-1)^u$ mutants. The replacement rate for such a transition is denoted $q_{k,u}$. For NBD evolutionary dynamics, this is given by

$$q_{k,u} = k(N - k) \left(s\beta_u w \frac{\delta_{1-u} + \gamma_{1-u,u}}{\delta_0 + \delta_1 + \gamma_{0,1} + \gamma_{1,0}} + \delta_{1-u} \frac{\beta_u}{\beta_0(N - k - u) + \beta_1(k - 1 + u)} \right).$$

The bias is then given by

$$r_k = \frac{q_{k,0}}{q_{k,1}}.$$

Appendix F. Showing strict order in bias for complete network

Here we want to show that equation (18),

$$r_k^{(i)} > r_k^{(ii)} > r_k^{(iii)},$$

holds for the complete network. From Table 3 we have

$$r_k^{(i)} = \frac{\beta_0}{\beta_1} \frac{(N - k - 1)\beta_0 + k\beta_1}{(N - k)\beta_0 + (k - 1)\beta_1}, \quad r_k^{(ii)} = \frac{\delta \frac{\beta_0}{y_k} + \beta_0 w \frac{1}{2}}{\delta \frac{\beta_1}{x_k} + \beta_1 w \frac{1}{2}}, \quad r_k^{(iii)} = \frac{\beta_0}{\beta_1}.$$

The denominator in all three cases is strictly positive because we are assuming that $\beta_0, \beta_1, \delta, N, k, w$ are strictly positive, and that $k \in \{1, \dots, N - 1\}$. Let

$$x_k = (N - k - 1)\beta_0 + k\beta_1 \quad \text{and} \quad y_k = (N - k)\beta_0 + (k - 1)\beta_1.$$

We then have that

$$\begin{aligned} r_k^{(i)} > r_k^{(ii)} &\Leftrightarrow \frac{\beta_0}{\beta_1} \frac{x_k}{y_k} > \frac{\delta \frac{\beta_0}{y_k} + \beta_0 w \frac{1}{2}}{\delta \frac{\beta_1}{x_k} + \beta_1 w \frac{1}{2}} \\ &\Leftrightarrow \beta_0 \beta_1 \left(\delta + \frac{w x_k}{2} \right) > \beta_0 \beta_1 \left(\delta + \frac{w y_k}{2} \right) \\ &\Leftrightarrow x_k > y_k \\ &\Leftrightarrow \beta_1 > \beta_0. \end{aligned}$$

Similarly, we have that

$$\begin{aligned} r_k^{(ii)} > r_k^{(iii)} &\Leftrightarrow \frac{\delta \frac{\beta_0}{y_k} + \beta_0 w \frac{1}{2}}{\delta \frac{\beta_1}{x_k} + \beta_1 w \frac{1}{2}} > \frac{\beta_0}{\beta_1} \\ &\Leftrightarrow \beta_0 \beta_1 \left(\frac{\delta}{y_k} + w \frac{1}{2} \right) > \beta_0 \beta_1 \left(\frac{\delta}{x_k} + w \frac{1}{2} \right) \\ &\Leftrightarrow x_k > y_k \\ &\Leftrightarrow \beta_1 > \beta_0. \end{aligned}$$

Since $r_k^{(i)} > r_k^{(ii)}$ and $r_k^{(ii)} > r_k^{(iii)}$, we have that $r_k^{(i)} > r_k^{(iii)}$. Therefore, equation (5.7) holds when $\beta_1 > \beta_0$, which we have assumed is true for an advantageous mutant invading a resident population.

Appendix G. Average fixation probability in star network

Here we show how to calculate the average fixation probability in the star network, where it is used in section 5.1.2. In the star network, we only consider population states with one individual on each site due to evolutionary dynamics being used. In such states, the position of residents and mutants present on leaves does not matter, since the leaves are identical. The population state is then given by (u, k) where u is the centre individual's type and k is the number of mutants on leaves ($N - 1 - k$ is the number of residents on leaves). Since $u \in \{0, 1\}$, in state (u, k) there are $1 - u \leq k \leq N - 1 - u$ mutants on the leaves provided that there is at least one mutant and resident in the population. Let $r(u, k, u', k')$ be the rate of transitioning from state (u, k) to (u', k') . We only need to consider the two transitions where a change in state occurs. First, for NBD evolutionary dynamics a type u centre can replace a type $1 - u$ leaf with rate

$$r(u, k, u, k - (-1)^u) = k^{1-u}(N - 1 - k)^u \left(sw_c \beta_u \frac{\delta_{1-u} + \gamma_{1-u,u}}{\delta_0 + \delta_1 + \gamma_{0,1} + \gamma_{1,0}} + \delta_{1-u} \right). \quad (\text{G.1})$$

Second, a type u centre is replaced by a type $1 - u$ leaf with rate

$$r(u, k, 1 - u, k) = k^{1-u}(N - 1 - k)^u \left(sw_l \beta_{1-u} \frac{\delta_u + \gamma_{u,1-u}}{\delta_0 + \delta_1 + \gamma_{0,1} + \gamma_{1,0}} + \delta_u \frac{\beta_{1-u}}{(N - 1 - k)\beta_0 + k\beta_1} \right). \quad (\text{G.2})$$

Using these rates, we can calculate the average fixation probability. In Hadjichrysanthou et al [25], the average fixation probability is given by

$$\bar{\rho}_{\text{star}} = \frac{\rho_{\text{star(centre)}} + (N - 1)\rho_{\text{star(leaf)}}}{N}.$$

Here, $\rho_{\text{star(centre)}}$ is the fixation probability of a mutant starting in the centre and $\rho_{\text{star(leaf)}}$ is the fixation probability of a mutant starting in a leaf. They are given by

$$\rho_{\text{star(centre)}} = \frac{p(1, 0, 1, 1)}{A(1, N - 1)} \quad \text{and} \quad \rho_{\text{star(leaf)}} = \frac{p(0, 1, 1, 1)}{A(1, N - 1)} \quad (\text{G.3})$$

where

$$A(l, m) = 1 + \sum_{j=l}^{m-1} p(1, j, 0, j) \prod_{k=l}^j \frac{p(0, k, 0, k - 1)}{p(1, k, 1, k + 1)}.$$

and

$$p(u, k, u, k - (-1)^u) = \frac{r(u, k, u, k - (-1)^u)}{r(u, k, u, k - (-1)^u) + r(u, k, 1 - u, k)},$$

$$p(u, k, 1 - u, k) = \frac{r(u, k, 1 - u, k)}{r(u, k, u, k - (-1)^u) + r(u, k, 1 - u, k)}.$$

For each of the cases considered, $\bar{\rho}_{\text{star}}$ is given by:

$$\bar{\rho}_{\text{star}}^{(i)} = \frac{\frac{1}{N} \frac{N-1}{N} + \frac{N-1}{N} \frac{\beta_1}{(N-2)\beta_0+2\beta_1}}{1 + \sum_{j=1}^{N-2} \frac{\beta_0}{(N-j)\beta_0+j\beta_1} \prod_{k=1}^j \frac{(N-k)\beta_0+k\beta_1}{(N-1-k)\beta_0+(k+1)\beta_1}},$$

$$\bar{\rho}_{\text{star}}^{(ii)} = \frac{\frac{1}{N} \frac{sw_c\beta_1/2+\delta}{s(w_c\beta_1+w_l\beta_0)/2+\delta} \frac{N}{N-1} + \frac{N-1}{N} \frac{sw_l\beta_1/2+\delta} {s(w_l\beta_1+w_c\beta_0)/2+\delta} \frac{\beta_1}{(N-2)\beta_0+\beta_1}}{1 + \sum_{j=1}^{N-2} \frac{sw_l\beta_0/2+\delta}{s(w_l\beta_0+w_c\beta_1)/2+\delta} \frac{\beta_0}{(N-1-j)\beta_0+j\beta_1} \prod_{k=1}^j \frac{sw_c\beta_0/2+\delta}{sw_c\beta_1/2+\delta} \frac{s(w_c\beta_1+w_l\beta_0)/2+\delta}{s(w_c\beta_0+w_l\beta_1)/2+\delta} \frac{(N-k)\beta_0+k\beta_1}{(N-1-k)\beta_0+(k+1)\beta_1}},$$

$$\bar{\rho}_{\text{star}}^{(iii)} = \frac{\frac{1}{N} \frac{w_c\beta_1}{w_c\beta_1+w_l\beta_0} + \frac{N-1}{N} \frac{w_l\beta_1}{w_l\beta_1+w_c\beta_0}}{1 + \sum_{j=1}^{N-2} \frac{w_l\beta_0}{w_l\beta_0+w_c\beta_1} \left(\frac{\beta_0}{\beta_1} \frac{w_c\beta_1+w_l\beta_0}{w_c\beta_0+w_l\beta_1} \right)^j}.$$

Appendix H. Proof for star network

Here we want to show that equation (18) holds for the star network when $N \rightarrow \infty$. In case (i) we have that

$$\lim_{N \rightarrow \infty} \bar{\rho}_{\text{star}}^{(i)} = 0.$$

In case (ii) we have that

$$\lim_{N \rightarrow \infty} \bar{\rho}_{\text{star}}^{(ii)} = \frac{\frac{w_l\beta_1}{w_l\beta_1+w_c\beta_0+2\delta}}{1 + \frac{w_l\beta_0}{w_l\beta_0+w_c\beta_1+2\delta} \sum_{j=1}^{\infty} \left(\frac{w_c\beta_0+2\delta}{w_c\beta_1+2\delta} \frac{w_c\beta_1+w_l\beta_0+2\delta}{w_c\beta_0+w_l\beta_1+2\delta} \right)^j}.$$

The denominator in this case converges to

$$1 + \frac{ar}{1-r}$$

where

$$a = \frac{w_l\beta_0}{w_l\beta_0+w_c\beta_1+2\delta},$$

$$r = \frac{w_c\beta_0+2\delta}{w_c\beta_1+2\delta} \frac{w_c\beta_1+w_l\beta_0+2\delta}{w_c\beta_0+w_l\beta_1+2\delta}.$$

Let

$$x = \frac{w_l\beta_1}{w_l\beta_1+w_c\beta_0+2\delta},$$

we therefore have that

$$\lim_{N \rightarrow \infty} \bar{\rho}_{\text{star}}^{(ii)} = \frac{x(1-r)}{1+r(a-1)}.$$

In case (iii) we have that

$$\lim_{N \rightarrow \infty} \bar{\rho}_{\text{star}}^{(\text{iii})} = \frac{x_{\delta=0}(1 - r_{\delta=0})}{1 + r_{\delta=0}(a_{\delta=0} - 1)}$$

where $x_{\delta=0}, a_{\delta=0}, r_{\delta=0}$ are x, a, r with $\delta = 0$. We have that

$$\lim_{N \rightarrow \infty} \bar{\rho}_{\text{star}}^{(\text{ii})} < \lim_{N \rightarrow \infty} \bar{\rho}_{\text{star}}^{(\text{iii})}$$

if $r > r_{\delta=0}, a < a_{\delta=0}, x < x_{\delta=0}$, which is indeed the case since $\beta_1 > \beta_0$ and $\delta > 0$ (in case (ii)). This therefore gives

$$\lim_{N \rightarrow \infty} \bar{\rho}_{\text{star}}^{(\text{i})} < \lim_{N \rightarrow \infty} \bar{\rho}_{\text{star}}^{(\text{ii})} < \lim_{N \rightarrow \infty} \bar{\rho}_{\text{star}}^{(\text{iii})}$$

as required.

Appendix I. Simulation Details

The Gillespie algorithm [21, 22] is used to simulate the evolutionary process described by the infinitesimal generator (equation (1)),

$$\begin{aligned} \mathcal{L}\phi(\mathcal{I}) &= \sum_{i \in \mathcal{I}} \sum_{n \in \mathcal{X}} [1 - \mu(i)] b(i, n, \mathcal{I}) [\phi(\mathcal{I} \cup \{(U_i, n)\}) - \phi(\mathcal{I})] \\ &\quad + \sum_{i \in \mathcal{I}} \sum_{n \in \mathcal{X}} \mu(i) b(i, n, \mathcal{I}) \int_{\mathbb{R}^l} [\phi(\mathcal{I} \cup \{(w, n)\}) - \phi(\mathcal{I})] M(U_i, w) dw \\ &\quad + \sum_{i \in \mathcal{I}} d(i, \mathcal{I}) [\phi(\mathcal{I} \setminus \{i\}) - \phi(\mathcal{I})]. \end{aligned}$$

Let T_k and I_k be the state of the population after k events have taken place. The following steps are followed for the simulation.

1. Determine the time, T_{k+1} , when a new event happens as follows,

$$T_{k+1} = T_k - \frac{\ln(\mathcal{U}(0, 1))}{\lambda_k}$$

where

$$\lambda_k = \sum_{i \in \mathcal{I}} \sum_{x \in \mathcal{X}} b(i, x, \mathcal{I}_k) + d(i, \mathcal{I}_k).$$

and $\mathcal{U}(0, 1)$ is a random number uniformly distributed in the range $(0, 1)$.

2. Determine the state, I_{k+1} , when a new event takes place:

- Birth without mutation: Individual i gives birth to an offspring of the same type onto site n with probability

$$[1 - \mu(i)] \frac{b(i, n, \mathcal{I}_k)}{\lambda_k},$$

then

$$I_{k+1} = I_k \cup \{(U_i, n)\}.$$

- Birth with mutation: Individual i gives birth to an offspring of type w onto site n with probability

$$\mu(i)M(U_i, w)\frac{b(i, n, \mathcal{I}_k)}{\lambda_k},$$

then

$$I_{k+1} = I_k \cup \{(w, n)\}.$$

- Death: Individual i dies with probability

$$\frac{d(i, \mathcal{I}_k)}{\lambda_k},$$

then

$$I_{k+1} = I_k \setminus \{i\}.$$

3. Repeat step 1 and 2 as necessary.

To solve the hitting probability (equation (12)),

$$\begin{cases} \mathcal{L}_c \rho(\mathcal{I}) = 0 & \mathcal{I} \notin \mathcal{M} \cup \mathcal{R}, \\ \rho(\mathcal{I}) = 0 & \mathcal{I} \in \mathcal{R}, \\ \rho(\mathcal{I}) = 1 & \mathcal{I} \in \mathcal{M}, \end{cases}$$

we set $T_0 = 0$ and $I_0 = \mathcal{I}$ such that $\mathcal{I} \notin \mathcal{M} \cup \mathcal{R}$, and then repeat steps 1 and 2 in the above algorithm until we hit a state in \mathcal{M} or \mathcal{R} . If we run N_{sim} simulations, out of which N_{mut} hit a state in \mathcal{M} , then the hitting probability is given by

$$\rho(\mathcal{I}) = \frac{N_{\text{mut}}}{N_{\text{sim}}}.$$

References

- [1] Allen, B., Lippner, G., Chen, Y.-T., Fotouhi, B., Momeni, N., Yau, S.-T. and Nowak, M. A. [2017], ‘Evolutionary dynamics on any population structure’, *Nature* **544**(7649), 227.
- [2] Allen, B. and Tarnita, C. E. [2014], ‘Measures of success in a class of evolutionary models with fixed population size and structure’, *Journal of mathematical biology* **68**(1-2), 109–143.
- [3] Berryman, A. [2003], ‘On principles, laws and theory in population ecology’, *Oikos* **103**(3), 695–701.
- [4] Beutel, A., Prakash, B. A., Rosenfeld, R. and Faloutsos, C. [2012], Interacting viruses in networks: Can both survive?, in ‘Proceedings of the 18th ACM SIGKDD International Conference on Knowledge Discovery and Data Mining - KDD ’12’, ACM Press, Beijing, China, p. 426.

- [5] Broom, M. and Rychtář, J. [2008], ‘An analysis of the fixation probability of a mutant on special classes of non-directed graphs’, *Proceedings of the Royal Society A: Mathematical, Physical and Engineering Sciences* **464**(2098), 2609–2627.
- [6] Champagnat, N., Ferrière, R. and Méléard, S. [2006], ‘Unifying evolutionary dynamics: From individual stochastic processes to macroscopic models’, *Theoretical Population Biology* **69**(3), 297–321.
- [7] Champagnat, N. and Lambert, A. [2007], ‘Evolution of discrete populations and the canonical diffusion of adaptive dynamics’, *The Annals of Applied Probability* **17**(1), 102–155.
- [8] Champagnat, N. and Méléard, S. [2007], ‘Invasion and adaptive evolution for individual-based spatially structured populations’, *Journal of Mathematical Biology* **55**(2), 147–188.
- [9] Constable, G. W. A. and McKane, A. J. [2015], ‘Models of Genetic Drift as Limiting Forms of the Lotka-Volterra Competition Model’, *Physical Review Letters* **114**(3), 038101.
- [10] Cremer, J., Melbinger, A. and Frey, E. [2011], ‘Evolutionary and Population Dynamics: A Coupled Approach’, *Physical Review E* **84**(5).
- [11] Czuppon, P. and Gokhale, C. S. [2018], ‘Disentangling eco-evolutionary effects on trait fixation’, *Theoretical Population Biology* **124**, 93–107.
- [12] Dieckmann, U. and Law, R. [1996], ‘The dynamical theory of coevolution: A derivation from stochastic ecological processes’, *Journal of Mathematical Biology* **34**(5-6), 579–612.
- [13] Durrett, R. [2009], ‘Coexistence in stochastic spatial models’, *The Annals of Applied Probability* **19**(2), 477–496.
- [14] Durrett, R. and Levin, S. [1996], ‘Spatial Models for Species-Area Curves’, *Journal of Theoretical Biology* **179**(2), 119–127.
- [15] Eames, K. T. D. and Keeling, M. J. [2002], ‘Modeling dynamic and network heterogeneities in the spread of sexually transmitted diseases’, *Proceedings of the National Academy of Sciences* **99**(20), 13330–13335.
- [16] Fisher, R. A. [1930], *The Genetical Theory of Natural Selection.*, Clarendon Press, Oxford.
- [17] Fournier, N. and Méléard, S. [2004], ‘A microscopic probabilistic description of a locally regulated population and macroscopic approximations’, *The Annals of Applied Probability* **14**(4), 1880–1919.
- [18] Frean, M., Rainey, P. B. and Traulsen, A. [2013], ‘The effect of population structure on the rate of evolution’, *Proceedings of the Royal Society of London B: Biological Sciences* **280**(1762), 20130211.
- [19] Frickel, J., Sieber, M. and Becks, L. [2016], ‘Eco-evolutionary dynamics in a coevolving host–virus system’, *Ecology Letters* **19**(4), 450–459.

- [20] Gerrish, P. J. and Lenski, R. E. [1998], The fate of competing beneficial mutations in an asexual population, *in* R. C. Woodruff and J. N. Thompson, eds, ‘Mutation and Evolution’, Vol. 7, Springer Netherlands, Dordrecht, pp. 127–144.
- [21] Gillespie, D. T. [1976], ‘A general method for numerically simulating the stochastic time evolution of coupled chemical reactions’, *Journal of computational physics* **22**(4), 403–434.
- [22] Gillespie, D. T. [1977], ‘Exact stochastic simulation of coupled chemical reactions’, *The journal of physical chemistry* **81**(25), 2340–2361.
- [23] Grenfell, B. T., Pybus, O. G., Gog, J. R., Wood, J. L., Daly, J. M., Mumford, J. A. and Holmes, E. C. [2004], ‘Unifying the epidemiological and evolutionary dynamics of pathogens’, *science* **303**(5656), 327–332.
- [24] Haafke, J., Abou Chakra, M. and Becks, L. [2016], ‘Eco-evolutionary feedback promotes Red Queen dynamics and selects for sex in predator populations’, *Evolution* **70**(3), 641–652.
- [25] Hadjichrysanthou, C., Broom, M. and Rychtář, J. [2011], ‘Evolutionary games on star graphs under various updating rules’, *Dynamic Games and Applications* **1**(3), 386.
- [26] Hanski, I. and Ovaskainen, O. [2003], ‘Metapopulation theory for fragmented landscapes’, *Theoretical Population Biology* **64**(1), 119–127.
- [27] Hanski, I., Schulz, T., Wong, S. C., Ahola, V., Ruokolainen, A. and Ojanen, S. P. [2017], ‘Ecological and genetic basis of metapopulation persistence of the Glanville fritillary butterfly in fragmented landscapes’, *Nature Communications* **8**, 14504.
- [28] Harris, T. E. [1974], ‘Contact Interactions on a Lattice’, *The Annals of Probability* **2**(6), 969–988.
- [29] Hindersin, L. and Traulsen, A. [2015], ‘Most Undirected Random Graphs Are Amplifiers of Selection for Birth-Death Dynamics, but Suppressors of Selection for Death-Birth Dynamics’, *PLOS Computational Biology* **11**(11), e1004437.
- [30] Hofbauer, J. and Sigmund, K. [1998], *Evolutionary Games and Population Dynamics*, Cambridge university press.
- [31] Holley, R. A. and Liggett, T. M. [1975], ‘Ergodic Theorems for Weakly Interacting Infinite Systems and the Voter Model’, *The Annals of Probability* **3**(4), 643–663.
- [32] Huang, W., Hauert, C. and Traulsen, A. [2015], ‘Stochastic game dynamics under demographic fluctuations’, *Proceedings of the National Academy of Sciences* **112**(29), 9064–9069.
- [33] Kao, K. C. and Sherlock, G. [2008], ‘Molecular characterization of clonal interference during adaptive evolution in asexual populations of *Saccharomyces cerevisiae*’, *Nature Genetics* **40**(12), 1499–1504.

- [34] Karlin, S. and Taylor, H. E. [1975], *A First Course in Stochastic Processes*, first edn, Academic Press, London.
- [35] Kaveh, K., Komarova, N. L. and Kohandel, M. [2015], ‘The duality of spatial death–birth and birth–death processes and limitations of the isothermal theorem’, *Royal Society open science* **2**(4), 140465.
- [36] Keeling, M. J. [2005], ‘Models of foot-and-mouth disease’, *Proceedings of the Royal Society B: Biological Sciences* **272**(1569), 1195–1202.
- [37] Kiss, I. Z., Green, D. M. and Kao, R. R. [2006], ‘The network of sheep movements within Great Britain: Network properties and their implications for infectious disease spread’, *Journal of The Royal Society Interface* **3**(10), 669–677.
- [38] Lee, B. Y., McGlone, S. M., Wong, K. F., Yilmaz, S. L., Avery, T. R., Song, Y., Christie, R., Eubank, S., Brown, S. T., Epstein, J. M., Parker, J. I., Burke, D. S., Platt, R. and Huang, S. S. [2011], ‘Modeling the Spread of Methicillin-Resistant *Staphylococcus aureus* (MRSA) Outbreaks throughout the Hospitals in Orange County, California’, *Infection Control & Hospital Epidemiology* **32**(6), 562–572.
- [39] Levins, R. [1969], ‘Some Demographic and Genetic Consequences of Environmental Heterogeneity for Biological Control’, *Bulletin of the Entomological Society of America* **15**(3), 237–240.
- [40] Lieberman, E., Hauert, C. and Nowak, M. [2005], ‘Evolutionary dynamics on graphs’, *Nature* **433**(7023), 312–316.
- [41] Maruyama, T. [1974], ‘A simple proof that certain quantities are independent of the geographical structure of population’, *Theoretical population biology* **5**(2), 148–154.
- [42] Matthews, L., Haydon, D. T., Shaw, D. J., Chase-Topping, M. E., Keeling, M. J. and Woolhouse, M. E. J. [2003], ‘Neighbourhood control policies and the spread of infectious diseases’, *Proceedings of the Royal Society of London. Series B: Biological Sciences* **270**(1525), 1659–1666.
- [43] Maynard Smith, J. [1982], *Evolution and the Theory of Games*, Cambridge university press.
- [44] Melbinger, A., Cremer, J. and Frey, E. [2010], ‘Evolutionary Game Theory in Growing Populations’, *Physical Review Letters* **105**(17).
- [45] Metz, J. A. J., Geritz, S. A. H., Meszena, G., Jacobs, F. J. A. and van Heerwaarden, J. S. [1995], ‘Adaptive Dynamics: A Geometrical Study of the Consequences of Nearly Faithful Reproduction’.
- [46] Möller, M., Hindersin, L. and Traulsen, A. [2019], ‘Exploring and mapping the universe of evolutionary graphs identifies structural properties affecting fixation probability and time’, *Communications Biology* **2**(1), 137.
- [47] Mollison, D. [1977], ‘Spatial contact models for ecological and epidemic spread’, *Journal of the Royal Statistical Society: Series B (Methodological)* **39**(3), 283–313.

- [48] Moran, P. A. P. [1959], ‘The survival of a mutant gene under selection’, *Journal of the Australian Mathematical Society* **1**(01), 121.
- [49] Moran, P. A. P. [1960], ‘The survival of a mutant gene under selection. II’, *Journal of the Australian Mathematical Society* **1**(04), 485.
- [50] Muller, H. J. [1932], ‘Some Genetic Aspects of Sex’, *The American Naturalist* **66**(703), 118–138.
- [51] Newman, M. E. J., Forrest, S. and Balthrop, J. [2002], ‘Email networks and the spread of computer viruses’, *Physical Review E* **66**(3).
- [52] Nowak, M. A., Sasaki, A., Taylor, C. and Fudenberg, D. [2004], ‘Emergence of cooperation and evolutionary stability in finite populations’, *Nature* **428**(6983), 646–650.
- [53] Ohtsuki, H., Hauert, C., Lieberman, E. and Nowak, M. A. [2006], ‘A simple rule for the evolution of cooperation on graphs and social networks’, *Nature* **441**(7092), 502–505.
- [54] Oksendal, B. [2013], *Stochastic Differential Equations: An Introduction with Applications*, Springer Science & Business Media.
- [55] Pattni, K., Broom, M., Rychtář, J. and Silvers, L. J. [2015], ‘Evolutionary graph theory revisited: When is an evolutionary process equivalent to the Moran process?’, *Proceedings of the Royal Society A: Mathematical, Physical and Engineering Sciences* **471**(2182), 20150334.
- [56] Patwa, Z. and Wahl, L. [2008], ‘The fixation probability of beneficial mutations’, *Journal of The Royal Society Interface* **5**(28), 1279–1289.
- [57] Pulliam, H. R. [1988], ‘Sources, Sinks, and Population Regulation’, *The American Naturalist* **132**(5), 652–661.
- [58] Rosenquist, J. N. [2010], ‘The Spread of Alcohol Consumption Behavior in a Large Social Network’, *Annals of Internal Medicine* **152**(7), 426.
- [59] Salathe, M., Kazandjieva, M., Lee, J. W., Levis, P., Feldman, M. W. and Jones, J. H. [2010], ‘A high-resolution human contact network for infectious disease transmission’, *Proceedings of the National Academy of Sciences* **107**(51), 22020–22025.
- [60] Shakarian, P., Roos, P. and Johnson, A. [2012], ‘A review of evolutionary graph theory with applications to game theory’, *Biosystems* **107**(2), 66–80.
- [61] Sharkey, K. J., Bowers, R. G., Morgan, K. L., Robinson, S. E. and Christley, R. M. [2008], ‘Epidemiological consequences of an incursion of highly pathogenic H5N1 avian influenza into the British poultry flock’, *Proceedings of the Royal Society B: Biological Sciences* **275**(1630), 19–28.
- [62] Tkadlec, J., Pavlogiannis, A., Chatterjee, K. and Nowak, M. A. [2019], ‘Population structure determines the tradeoff between fixation probability and fixation time’, *Communications Biology* **2**(1), 138.

- [63] Wells, C. R., Sah, P., Moghadas, S. M., Pandey, A., Shoukat, A., Wang, Y., Wang, Z., Meyers, L. A., Singer, B. H. and Galvani, A. P. [2020], ‘Impact of international travel and border control measures on the global spread of the novel 2019 coronavirus outbreak’, *Proceedings of the National Academy of Sciences* **117**(13), 7504–7509.
- [64] Wright, S. [1949], ‘The Genetical Structure of Populations’, *Annals of Eugenics* **15**(1), 323–354.
- [65] Zukewich, J., Kurella, V., Doebeli, M. and Hauert, C. [2013], ‘Consolidating birth-death and death-birth processes in structured populations’, *PLoS One* **8**(1), e54639.